PhD degree in Systems Medicine

Curriculum in Molecular Oncology

European School of Molecular Medicine (SEMM),

University of Milan and University of Naples "Federico II"

Settore disciplinare: BIO/11

Dissecting the STING-dependent molecular mechanisms in a preclinical model of combined treatment with tumour-targeted *Herpes simplex* virus and immune checkpoint blockade

Guendalina Froechlich

CEINGE, Naples

Matricola n. R12090

Supervisor: Prof. Nicola Zambrano, Ceinge, Napoli

Internal Supervisor: Prof. Achille Iolascon, Ceinge, Napoli

External Supervisor: Prof. Fabio Grassi, Institute for Research in Biomedicine, Bellinzona, Switzerland

Academic year 2020-2021

Table of contents

List of Abbreviations

Adoptive T Cell transfer therapy (ATC)

Antibody-Dependent Cellular Cytotoxicity (ADCC)

Antigen Presenting Cell (APC)

Bacillus Calmette-Guérin (BCG)

Chimeric Antigen Receptor (CAR-T)

C-type Lectin Receptors (CLRs)

Cyclic GMP–AMP (cGAMP)

Cyclic GMP–AMP Synthase (cGAS)

Cytotoxic T Lymphocyte Antigen 4 (CTLA4)

Dendritic cells (DCs)

European Medicines Agency (EMA)

Food and Drug Administration (FDA)

Granulocyte-Macrophage Colony-Stimulating Factor (GM-CSF)

Heperan Sulfate (HS)

Herpes Simplex Virus (HSV)

Herpes Virus Entry Mediator (HVEM)

High-Mobility Group Box 1 (HMGB1)

Human TElomerase Reverse Transcriptase (hTERT)

IFN Stimulated Genes (ISG)

Immune Checkpoint Inhibitors (ICI)

Immunogenic Cell Death (ICD)

Interferon Stimulatory DNA (ISD)

InterFeron-γ (IFNγ)-Inducible protein 16 (IFI16)

Lactate DeHydrogenase (LDH)

Mitochondrial AntiViral Signalling protein (MAVS)

Monoclonal AntiBodies (mAb)

NOD-Like Receptors (NLRs)

Oncolytic HSV (oHSV)

Oncolytic Viruses (OV)

Pathogen-Associated Molecular Patterns (PAMPs)

Pattern Recognition Receptors (PRRs)

Programmed Death 1 (PD-1)

Protein Kinase R (PKR)

RIG-I-Like Receptors (RLRs)

STimulator of INterferon Genes (STING)

T Cell Receptor (TCR)

T Regulatory (Treg)

Talimogene laherparepVEC (T-VEC)

Toll-Like Receptors (TLRs)

Transcripts Per Kilobase Million (TPM)

Tumour Associated Antigens (TAA)

Tumour Infiltrating Lymphocytes (TILs)

Unique Long (Ul)

Unique Short (Us)

Figure Index

1. Abstract

Oncolytic viruses promote anti-tumour immune response by direct tumour cell killing and activation of intratumoural immune system. The role of innate antiviral immune response to oncolytic viruses is still debated, as they counteract viral replication and trigger adaptive antitumor immunity. The DNA sensing-mediated cGAS/STING axis may act as a key balancer between lytic and immunotherapeutic activity of oncolytic viruses. Indeed, upon infection, viral DNA is sensed by cGAS/STING axis that, in turn, induces type-I interferon cascade counteracting viral replication and spread. For this reason, STING represents a hurdle for classical lytic-centric function of oncolytic viruses. On the other side, the immunological role of STING should also be considered, as it is emerging as a key bridge between innate and adaptive immunity. To evaluate the role of STING expression in tumour cells in response to onco-virotherapy, we generated murine STING KO tumour cell lines through CRISPR/Cas9 genome editing. Preclinical studies in syngeneic immunocompetent tumour-bearing mice showed that the inactivation of STING in tumour cells, while favouring oncolytic viral replication, impaired the immunotherapeutic effects of combination therapy based on herpetic oncolytic virus and PD1 blockade. Molecular characterization of tumours revealed that loss of STING prevents antitumour immune activation inducing a tolerogenic cell death and immunosuppressive tumour microenvironment. Accordingly, I propose that antiviral, tumour-resident STING provides fundamental contributions to heat-up the TME eliciting immunotherapeutic efficacy of oncolytic viruses.

2. Introduction

2.1. Cancer Immunotherapy

Cancer immunotherapy is considered the "fifth pillar" of cancer therapy with surgery, chemotherapy, radiotherapy and targeted therapy [1]. It has been known from decades that there is a tight interplay between cancer and immune system named cancer immunoediting [2]. This mechanism can be divided into 3 phases: Elimination – Equilibrium – Escape. Each day, thousands of mutations can occur in normal cells as the result of exposure to DNA-damaging agents and genome replication. In most cases, DNA repair mechanisms that are activated in the presence of DNA alterations can efficiently cope with the occurrence of damages [3]. If DNA damages are not repaired in a timely manner, or are too extensive to be repaired, intracellular pathways can drive cell death [4]. If these mechanisms are altered, cells can acquire distinct features that can lead to malignant transformations. At this point, elimination phase starts as immune system can join the game by recognition and killing of these altered cells. The mechanisms by which these cells with potential of malignant transformation are recognized rely on membrane protein pattern alteration that activates NK cells as well as display of non-self antigens recognized by cytotoxic T cells. These non-self antigens origin from somatic non-synonymous mutations (point missense mutations and indel mutations altering the open reading frame) occurring in the coding sequences of genes. Sporadic transformed cells can escape the *Elimination phase* progressing into *Equilibrium phase*. During this phase, under the selective pressure of immune system, pre-transformed cells can acquire additional hits of mutations and epigenetic alteration leading to limited growth and cellular immunogenicity. The constant immunoediting pressure can lead to the *Escape phase*, in which the cells acquire features that definitely allow them to escape immune system and to grow in an unrestricted manner, by inducing an immunosuppressive microenvironment. The goal of cancer immunotherapy is to reverse this process to elimination phase or, as an alternative, to render cancer a chronic disease (Figure 1) [5].

To date, cancer immunotherapy relies on different approaches, as described below:

- **Immune checkpoint therapy.** Checkpoint molecules tightly regulate the action of T cells, leading to an activation and repression balance stimuli. Naïve T cells display T Cell Receptors (TCR) on their surface for the interaction with the antigen, loaded on MHC molecules expressed by Antigen Presenting Cells (APC). The latter, moreover, display co-stimulatory molecules (B7-1/B7-2) that interact with CD28 molecule on T cells; this is necessary for the full activation of naïve T cells. The interaction between TCR/MHC I-II and co-stimulatory molecules represents the immunological synapse [6]. Early after

activation, in lymphoid tissues, T cells begin to display on their surface the inhibitory molecule Cytotoxic T Lymphocyte Antigen 4 (CTLA4) and Programmed Death 1 (PD-1) that can anergize lymphocytes by interaction with the respective ligands B7-1/B7-2 and PD-L1/PD-L2, respectively. In the same context, CTLA4 is constitutively expressed by T Regulatory (Treg) cells, that contribute to sequestering of CD28 co-stimulatory activity. Additional inhibitory molecules contribute to turn off the immune activation (LAG-3, TIM-3, TIGIT), overcoming the stimulatory ones (OX40, 4-1BB) and leading to an immunocompromised TME and to the escape phase of cancer immunoediting [7-9]. CTLA4 and PD-1 molecules have been extensively targeted by immunotherapeutic treatments leading to unprecedented antitumor efficacy, thus, their discovery allowed James P. Allison and Tasuku Honjo to be awarded of Nobel Prize 2018 in Physiology or Medicine. Many different monoclonal antibodies (mAb_s) have been developed to interfere with CTLA4/CD28 and PD-1/PDL1-2 interactions. Additional antitumor mechanisms of action have been described, including Treg depletion by antiCTLA4-mediated antibody-dependent cellular cytotoxicity (ADCC) and co-stimulus reactivation by PD-1 targeting [10]. To date, Food and Drug Administration (FDA) and European Medicines Agency (EMA) have approved mAbs targeting the immunosuppressive receptors CTLA4 (Ipilimumab), PD1 (Nivolumab and Pembrolizumab) and PDL1 (Atezolizumab, Durvalumab and Avelumab) [11-12]. Despite unprecedent response to Immune Checkpoint Inhibitors (ICI) therapy, the anti-tumour efficacy is still restricted to a limited percentage of patients, due to intrinsic and acquired mechanisms of resistance, suggesting the need for combination therapy [13-14]. Based on these considerations, the promising therapy are the combination with the well-characterised inhibitory mAbs with secondary inhibitory/co-stimulatory targets reactivating T cells anergy from several fronts [15].

- **Adoptive T cell transfer therapy.** Adoptive T Cell transfer therapy (ATC) consists of isolation, *ex vivo* expansion (with IL-2 supplement) and reinfusion of Tumour Infiltrating Lymphocytes (TILs) [16] or engineering of peripheral T cells with a Chimeric Antigen Receptor (CAR-T) targeting a surface tumour antigen. The 1^{st} generation CAR receptor is assembled by fusing antibody fragments to intracellular CD3-zeta (ζ). Next generations CAR (up to 4^{th} generation) have been further improved by fusing additional costimulatory domains and intracellular moieties to improve proliferation, cytotoxicity and survival of transduced CAR-T cells. The FDA approved in 2017 the use of CAR-T treatment for refractory B-cell acute lymphoblastic leukaemia in paediatric patients.
- **Cancer vaccines.** Cancer vaccines act as enhancers of immune system to fight cancer and are classified as prophylactic and therapeutic. The approved prophylactic vaccines

are exploited for the prevention of Hepatitis B Virus and Human Papilloma Virus infections, being able to cause hepatic carcinoma and cervical cancer, respectively. In contrast to prophylactic vaccines that are able to prevent oncogenic virus-mediated cancer in almost 100% of cases, therapeutic ones are more challenging due to immunocompromised TME and systemic immune anergy. Moreover, therapeutic vaccines targeting tumour associated antigens (TAA) and neoantigens are often poorly immunogenic, due to their self-origin and high degree of identity to wild-type proteins [17]. To overcome a “cold” TME, therapeutic cancer vaccines are often combined with immune checkpoint inhibitors acting as boost for resident anti-tumour T cells [18]. Another class of therapeutic cancer vaccines are represented by endovaccines including oncolytic viruses described in next session.

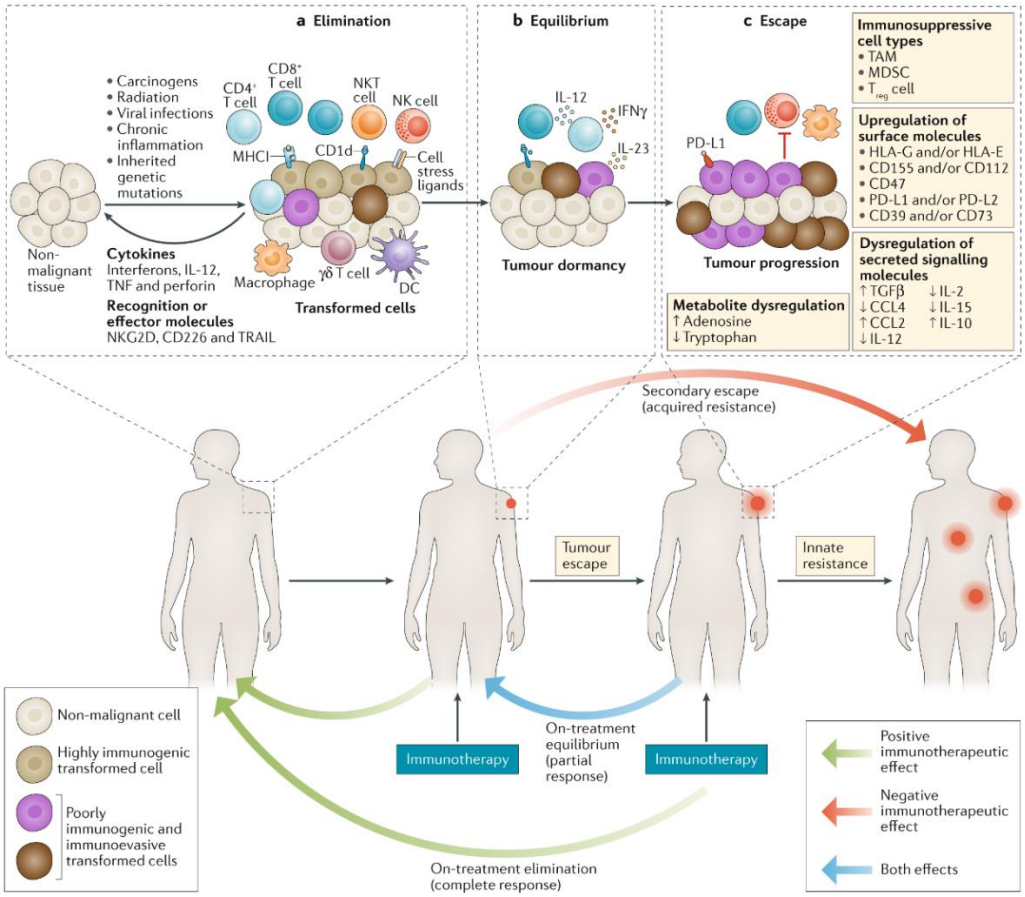

Figure 1. Cancer immunoediting: Elimination – Equilibrium – Escape. (A) During the elimination phase, the innate and adaptive immune systems recognize transformed cells and eliminate them before they become clinically detectable. (B) Tumour cells that survive the elimination phase can progress into the equilibrium phase, in which they acquire additional mutations leading to a limited growth and cellular immunogenicity. (C) Edited tumours can enter escape phase, in which their growth is uncontrolled and become clinically detectable; this phase is characterised by an activation of immunosuppressive and/or immunoevasive pathways. Effective immunotherapy can drive tumours back to the elimination phase leading to complete response. Alternatively, if the immunotherapy completely does not overcome tumour-induced immune suppression, the tumour regress into on-treatment equilibrium, characterized by a partial response. Selected tumour cell clones are able to evade or suppress antitumour immunity resulting in secondary escape, characterized by an acquired resistance to therapy [19].

2.2. Oncolytic Viruses

Based on the idea that immune system can play a major role in neoplastic development, the use of microbes as antitumour drugs has been developed. The first report of significant shrinkage of tumours after intentional infection of a cancer patient with *Erysipelas* was reported in 1868 by Wilhelm Busch [20]. In 1976, when the administration of live attenuated bacterium *Bacillus Calmette-Guérin* (BCG) resulted effective for the treatment of a bladder tumour, the idea that antiviral immune system can support antitumor immunity started to spread within scientific community [21]. The first engineered virus implemented as oncolytic was a thymidine kinase-negative mutant of *Herpes simplex* Virus (HSV); after few years, a second oncolytic vector was engineered, based on an adeno virus mutant [22-23]. In the last 20 years, more than 100 independent clinical trials using oncolytic viruses have been reported, leading to the approval by FDA in 2015 of Talimogene laherparepvec (T-VEC), an attenuated HSV-1 encoding granulocyte-macrophage colony-stimulating factor (GM-CSF) for the local treatment of metastatic malignant melanoma [24]. After years of debates, oncolytic viruses (OV) have been accepted as considerable class of immunotherapeutic drugs for cancer treatments. Indeed, the classical view of onco-virotherapy relying on selective killing of tumour cells has been resized, opening to a more immune-centric view of OV's mechanism of action. Indeed, despite initial tumour regression is mediated by OV-mediated direct killing, the predominant contribution is mediated by Immunogenic Cell Death (ICD) activation and host anti-tumour immunity stimulation. For these reasons, oncolytic viruses are considered as cancer vaccines with multi-mechanistic antitumor actions, able to trigger positive feedbacks activating both innate and adaptive anti-tumour immunity [25]. As result of OV-mediated tumour cell lysis, Pathogen-Associated Molecular Patterns (PAMPs) are massively released into the TME triggering to the activation of Pattern Recognition Receptors (PRRs). This event culminates in the release of type I interferons (IFN-α/β) mainly from tumour infected cells that, in turn, stimulates the secondary secretion of inflammatory mediators from bystander cells. These molecules include stimulating cytokines, such as IL-1, IL-6, IL-12, IL-18, IFN-γ, GM-CSF, TNF-α, and chemokines, such as CCL2 and CCL5, triggering an inflammatory cascade. In this way, both innate and adaptive immune cells are recruited and activated into the TME. Among others, infected tumour cells also release tumour antigens (tumour associated antigens, TAA; neoantigens) that are engulfed, processed, and presented by antigen presenting cells. Tumour antigens presented in this immune-proficient microenvironment can effectively activate naïve and pre-existing anergic antitumor T cells. Dendritic cells (DCs) also migrate in lymph drawing lymph nodes where they can present both tumour and viral antigens to helper T cells (CD4+) that, in turn, promote B cells and CD8+ T cells activation and differentiation. Despite the role of

antiviral adaptive immunity is still debated, it is widely accepted from scientific community that antiviral T cells can be beneficial for antitumor immunity by presenting viral antigens in an antitumour-antiviral shared immunological synapse, thus reinforcing cytotoxic potential of both antitumor CD8+ T and NK cells [26]. These are the principal OV mechanisms of action in which there is a tripartite action of direct oncolytic virus cell killing, activation/re-activation of anti-tumour immune response with a strong synergy of OV-induced antiviral immunity that transmute an immunocompromised TME in an immunocompetent one. Finally, such oncolytic viruses can host transgenes of interest to enhance antitumor efficacy. These latter are usually immunomodulators to further recruit or activate intratumour adaptive immunity (Figure 2).

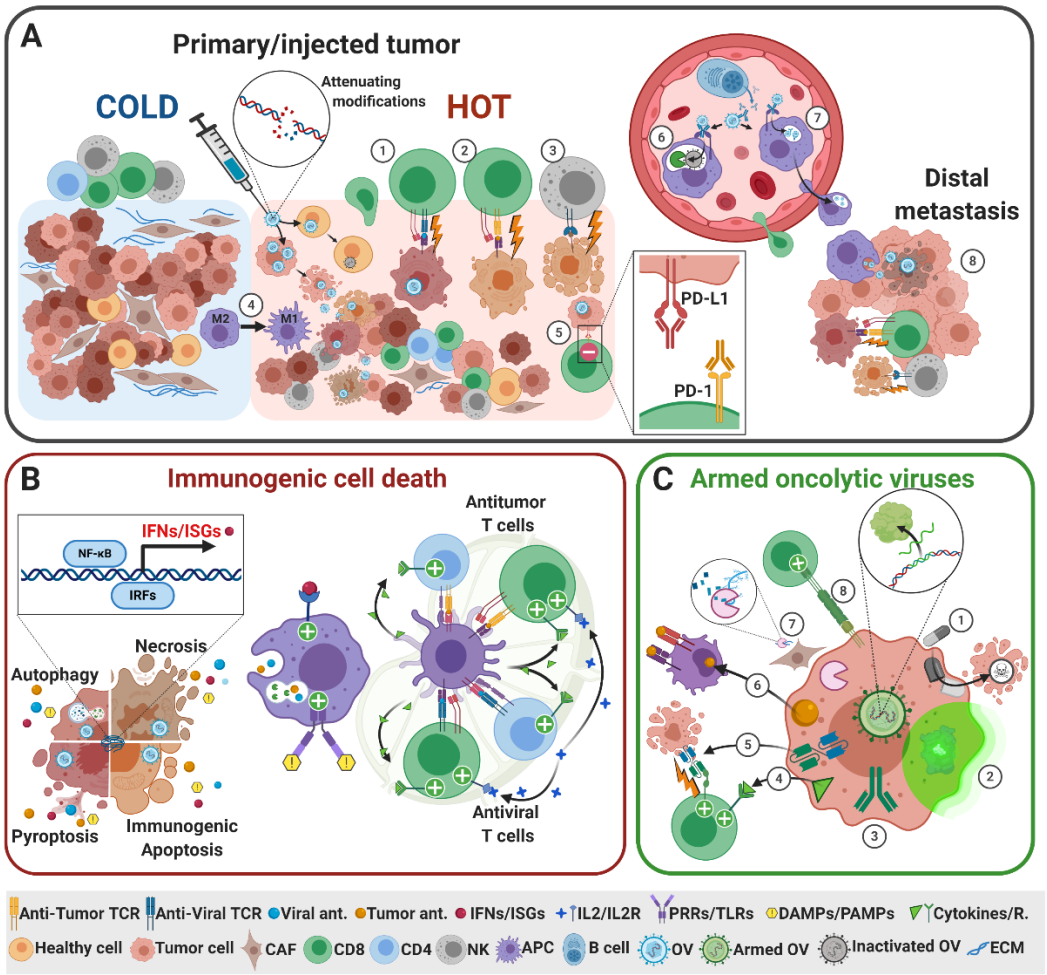

Figure 2. The multi-mechanistic antitumor actions of oncolytic viruses. (A) The direct injection of oncolytic viruses in primary/accessible tumours induces the lysis of tumour cells, sparing healthy ones; the recruitment of immune cells is promoted within "cold" tumour microenvironment. (B) Immunogenic cell death (ICD) is the core activity of OVs. ICD leads to the activation of antiviral innate immunity (type I IFNs and ISGs), release of DAMPs, PAMPs, exposure of viral and tumour antigens. Tumour resident APCs can capture these molecules and present antigens into the lymph nodes, activating both antiviral and antitumor T cells. In turns, adaptive antiviral immune response can synergize with antitumour immune response by helper T cells activity and by killing virus-infected cells. (C) The antitumour activity of OVs can be enhanced by arming viral genomes with payloads [27].

2.2.1. HSV-1 as Oncolytic Virus

Herpes simplex Virus Type 1 is among the most used vector implemented as an oncolytic virus. HSV-1 is a dsDNA virus with a genome size up to 150kb, divided in two unique sequences, unique long (Ul) and unique short (Us), flanked by inverted repeats. Starting from the external layer, HSV-1 is structured by an envelope coated with glycoproteins required for viral entry (gB, gC gD, gH/L); the tegument, comprising of proteins helpful for viral entry, capsid transport, and immediate early phase of transcription; the icosahedral capsid, containing the viral genome (Figure 3) [28]. The mechanism of HSV-1 entry involves envelope glycoproteins with a first interaction between Heperan Sulfate (HS) and viral glycoprotein gC. The binding of gD to *Herpes* Virus entry mediator (HVEM) and Nectin-1 stabilise the first weak interaction. Eventually, gH/gL complex mediates the host and viral membrane fusion to allow the capsid to migrate towards the nucleus through the microtubules and release the viral genome (Figure 4) [29-31]. The development of HSV-1 as oncolytic vector (oHSV) has several advantages including: (i) easy access to manipulate and insert multiple transgenes; (ii) infecting several malignant cell types with quick replication in the infected cells; (iii) existing of specific antiviral agents to terminate HSV replication in case of serious adverse effects (Acyclovir & Ganciclovir) [32]. The main disadvantage is the high prevalence of HSV-1 infection throughout the population that could limit the viral replication, due to a pre-existing immunity and neutralising antibodies. The most implemented genetic modifications to make HSV-1 selective for tumour cells sparing normal cells are described below:

- **Attenuated.** Genome attenuation can be obtained by mutation or deletions in one or more genes essential for virulence. The central limitation of these OVs is the attenuation of virulence in both normal and in tumour cells, thus limiting oncolysis. The first example of attenuating mutations is *UL39* gene, encoding ribonucleotide reductase ICP6, that is required for DNA synthesis. Oncolytic HSV ΔICP6 can replicate only in cells with high proliferative rate able to complement the lacking ribonucleotide reductase activity including tumour cells. The second example, $\gamma_1 34.5$ gene is present in double copy and encodes for ICP34.5 protein. Protein Kinase R (PKR) is a protein activated by healthy cells in response to viral infection. PKR inactivates by phosphorylation, the translation initiation factor eIF2α, thus arresting protein synthesis. During HSV-1 infection, ICP34.5 protein recruits phosphatase 1, reactivating eIF2α and protein synthesis. Since IFN pathway is often impaired in cancer, the $\Delta\gamma_1 34.5$ oHSVs replicate only in tumour cells, whereas

abortive replication cycle occurs in healthy tissues. Most of HSV-based oncolytic viruses, including T-VEC harbour this mutation (Figure 5) [33].

- **Transcriptionally retargeted (TR).** One or more viral genes can be modified in transcriptional control by inserting tumour related promoter elements upstream viral coding sequence to get selective transcription and viral propagation in cancer cells. This approach has been exploited in clinical stage oHSV rQNestinHSV-1 expressing ICP34.5 under control of Nestin promoter [34] and oHSV1-hTERT expressing the essential gene ICP4 under the control of human TElomerase Reverse Transcriptase (hTERT) gene promoter [35]. The combination of such approaches can also be implemented to get a more stringent viral restriction to tumour cells (Figure 5) [36].
- **Tropism retargeted.** This approach exploits the viral entry to achieve tumour selectivity. As previously described, herpesviruses entry in host cells is mediated by membrane glycoproteins. The engineering of these class of OVs relies on de-targeting/re-targeting approaches through glycoproteins engineering. Essential moiety of viral glycoprotein can indeed be replaced with peptide ligands, or antibody fragments targeting a tumour surface antigen (Figure 5). With this approach Campadelli-Fiume and colleagues isolated non-attenuated, fully retargeted OVs targeting human HER2, demonstrating a significant preclinical efficacy (Figure 6) [37].

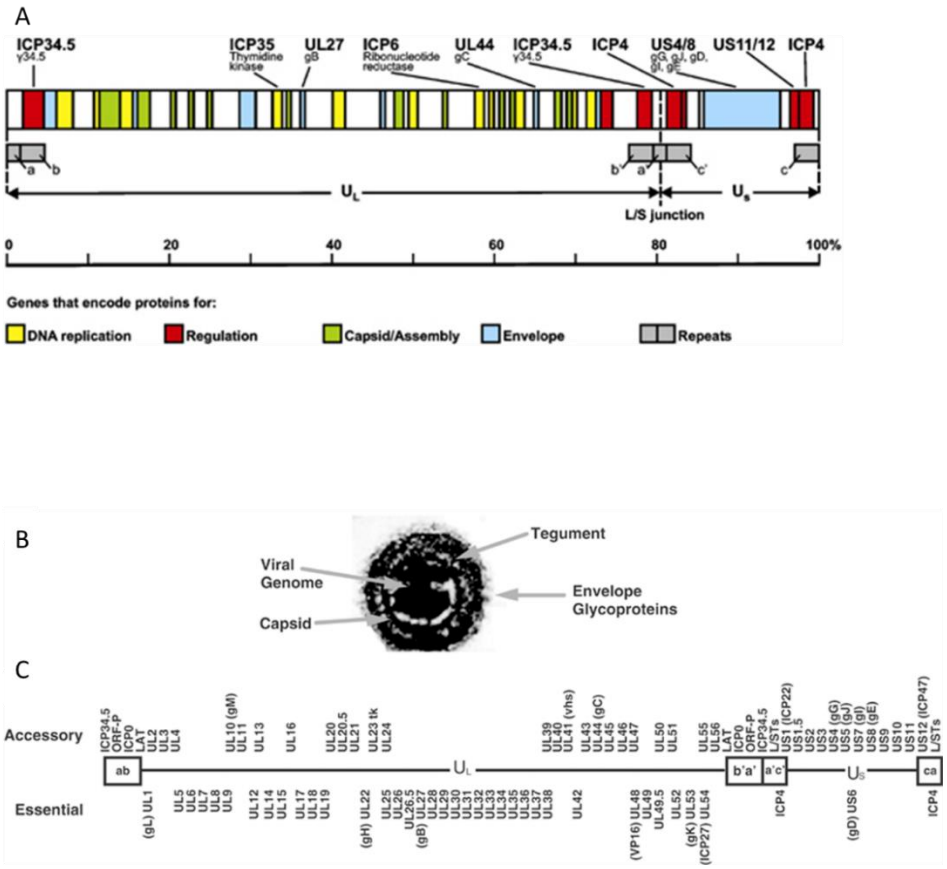

Figure 3. Schematic representation of HSV-1 genome. (A) The cartoon shows the genes involved in DNA replication (yellow), regulation (red), viral assembly (green for capsid and light blue for envelope proteins) and repeats regions (grey). (B) The image shows the physical structure of a HSV-1 viral particle. Starting from the inner the arrows indicate the viral genome, tegument, capsid and envelope glycoproteins. (C) The image shows the list of HSV gene, in details the distribution of Accessory (on top) and Essential (on bottom) genes. The essential genes are necessary for the replication *in vitro*, on contrary, the accessory genes can be deleted without influence the replication *in vitro*. In parenthesis there are the genes encoding glycoproteins and involved in pathogenesis [38-39].

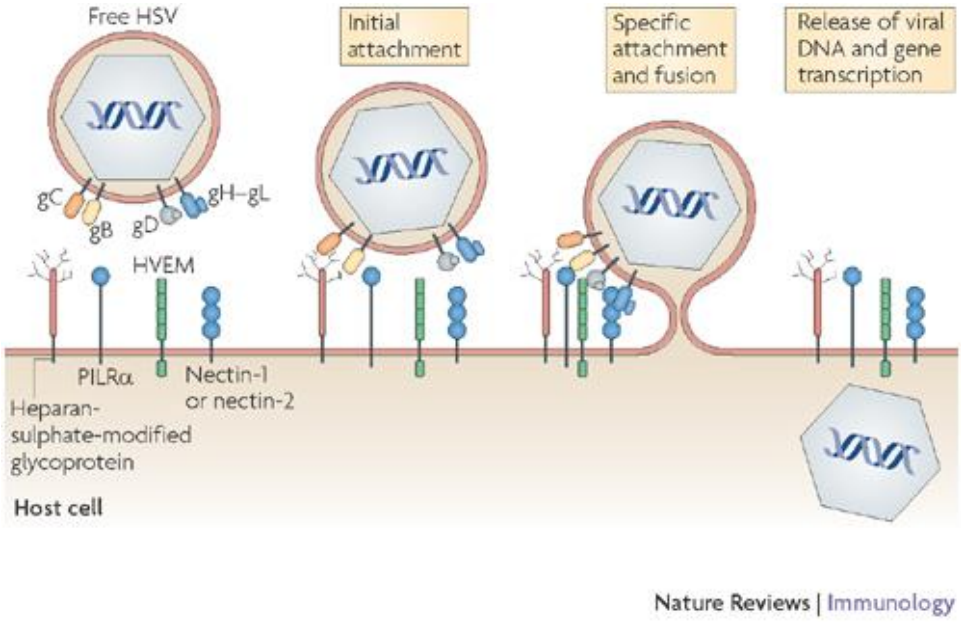

Figure 4. Herpes simplex virus entry receptors and ligands. HSV contains on its surface five glycoproteins that are used for its entry into host cells. gB and gC mediate the initial attachment of virus particles to heparan-sulphate-modified glycoprotein. gB binding to paired immunoglobulin-like type 2 receptor-α (PILRα) and gD binding to herpesvirus entry mediator (HVEM), nectin-1, nectin-2 or 3-O-sulphotransferase-modified heparan sulphate trigger membrane fusion and release of the viral nucleocapsid into the host-cell cytoplasm [40].

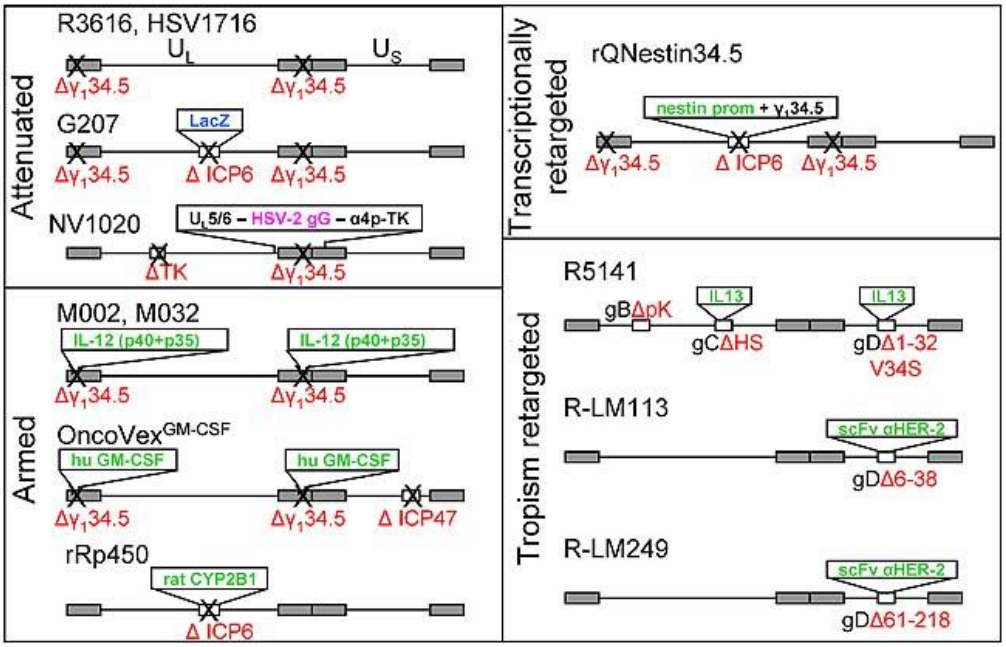

Figure 5. Schematic image of genetically engineered o-HSVs, grouped according to different strategies. (Attenuated) Defined as conditional replication oHSV, the engineering consists in deletion of viral genes that counteract the IFN-mediated PKR response, or genes essential for efficient viral replication in non-dividing cells. (Armed) The engineering consists in arming the oHSV with cytokines to improve tumour clearance. (Transcriptionally retargeted) One or more viral genes can be engineered by inserting tumour related promoter elements upstream viral coding sequence to get selective transcription and viral propagation in cancer cells. (Tropism retargeted) The oHSV no longer infects the natural target cells (de-targeting), but specifically infect the tumour cells with tumour specific receptors (retargeting) [41].

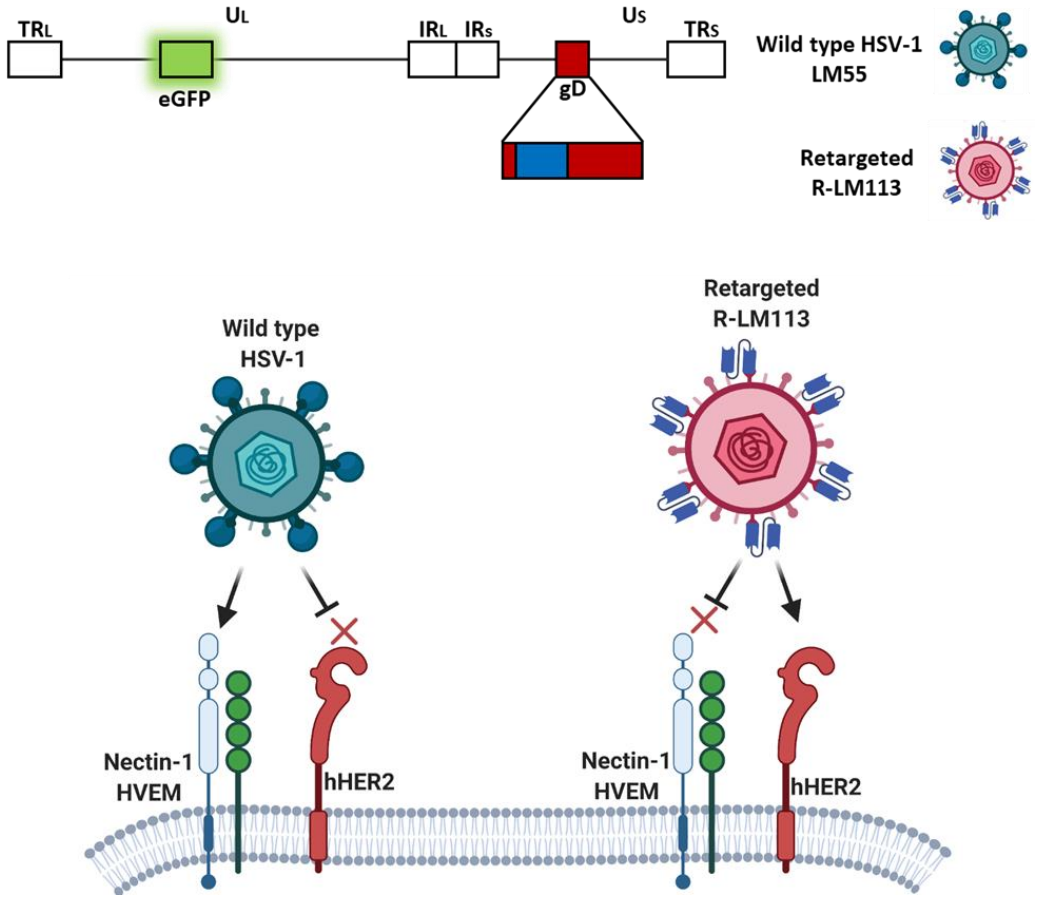

Figure 6. Representation of retargeting strategy of R-LM113 oHSV. Viral envelope glycoproteins that bind to widespread cellular receptors are modified to eliminate natural receptor binding and incorporate ligands or single-chain antibodies (scFv) that recognize tumour selective receptors. In detail in R-LM113 oHSV, Trastuzumab derived scFv have been introduced into the HSV gD genes to achieve retargeting. That leads to obtain a complete virus retargeting producing entry of cells solely via the novel receptor target and not via natural receptors.

2.2.2. Combination Therapy

The limited anti-tumour efficacy of OVs and immune checkpoint modulators suggests the need for combination therapy. As described before, ICI therapy is effective in a limited percentage of patients, due to an immunocompromised TME. On the other side, oncolytic virotherapy is able to turn “cold” tumours into “hot” ones, mostly thanks to the cooperation of the immune system. According to these observations, preclinical models and clinical trials have been developed to get full advantage from OVs and ICI therapies. To date, many clinical phases I to II trials have demonstrated superior efficacy of OV+ICI combination treatment, compared to monotherapies, paving the way to clinical approval in the next future [42].

2.3. Nucleic Acid Sensing

The innate immune response is responsible for recognition of viruses and microorganisms through specific sensors, called pattern recognition receptors (PRRs) [43]. The PRRs specifically recognize parts of pathogens named pathogen-associated molecular patterns (PAMPs), including glycoproteins and nucleic acids. We can distinguish PRRs expressed by professional immune cells and those widespread ubiquitously expressed. The Toll-like receptors (TLRs) and the C-type lectin receptors (CLRs) are expressed in macrophages and dendritic cells, mainly on plasma membrane or in endosomal compartments [44]. Among PRRs ubiquitously expressed are NOD-like receptors (NLRs), RIG-I-like receptors (RLRs) and a group of intracellular DNA sensors such as cyclic GMP–AMP synthase (cGAS) and interferon-γ (IFNγ)-inducible protein 16 (IFI16) [45]. Nucleic acids are one of the most important class of PAMPs. Both RNA and DNA can indeed activate distinct PRRs to alert cells in the presence of intracellular pathogens. While exogenous RNA is sensed by many PRRs with partially redundant functions, cGAS is essential to sense the presence of cytosolic DNA. Following the recognition of exogenous nucleic acids, PRRs activate intracellular pathway cascades by second messengers, such as stimulator of IFN genes (STING), MYD88 or mitochondrial antiviral signalling protein (MAVS). These pathways converge into the production of pro-inflammatory cytokines and chemokines and host defence molecules, in particular type I IFNs. Ultimately, secreted IFNs act in autocrine and paracrine manner, inducing the transcription of IFN stimulated genes (ISG), crucial for the amplification of anti-viral state [46]. The activation of PRR signalling, in turn, promotes the activation of adaptive immune response in order to neutralise viral infections.

2.3.1. STING DNA Sensing and HSV

It is well established that cGAS is the most characterised intracellular sensor of viral DNA. In the cytoplasm, viral dsDNA derived from DNA-based virus or retrovirus is sensed by cGAS.

The binding by DNA activates the cGAS catalytic activity inducing the production of 2'3' cyclic GMP–AMP (cGAMP), a potent agonist of STING. In addition, cGAMP from infected cells is capable to spread through gap junctions in neighbouring cells, thus, mediating STING activation and hampering viral infection. After a relevant conformational change due to cGAMP binding, STING protein is further activated by dimerization and is ubiquitylated by TRIM32 and TRIM56 translocating from endoplasmic reticulum to the Golgi apparatus. Furthermore, STING recruits TBK1, inducing its autophosphorylation, and the latter phosphorylates STING and recruits IRF3. The phosphorylation of IRF3 by TBK1 leads to its translocation into the nucleus inducing type I IFN gene expressions. At the same time, TBK1 induces the activation and translocation of NF-kB promoting inflammatory mediators' production (Figure 7) [47]. Viruses have evolved effective mechanisms to avoid detection by innate immune sensors, or to inhibit the activation of PRRs and/or their downstream signalling cascades. In particular, HSV-1 evolved a large number of mechanisms to hamper STING pathway at each step of its activation (Figure 8). The cGAS-STING pathway is activated at early stage of viral infection, for this reason VP22 viral protein is expressed at early time points post infection to counteract cGAS activity. Also UL37 tegument protein acts at upstream steps, deaminating cGAS and blocking, in turn, cGAMP production. $\gamma_1$34.5 viral protein is responsible to facilitate viral replication, hampering the arrest of translational machinery upon infection. In addition, ICP34.5 via its N-terminal domain binds TBK1 counteracting its activity. VP11/12 proteins act directly on STING degradation blocking the signalling. At downstream steps, UL42 interacts with NF-κB preventing its nuclear translocation, while VP16 protein prevents IRF3 transcription. These examples provide clear evidence of a complex interplay during human and HSV-1 co-evolution [48].

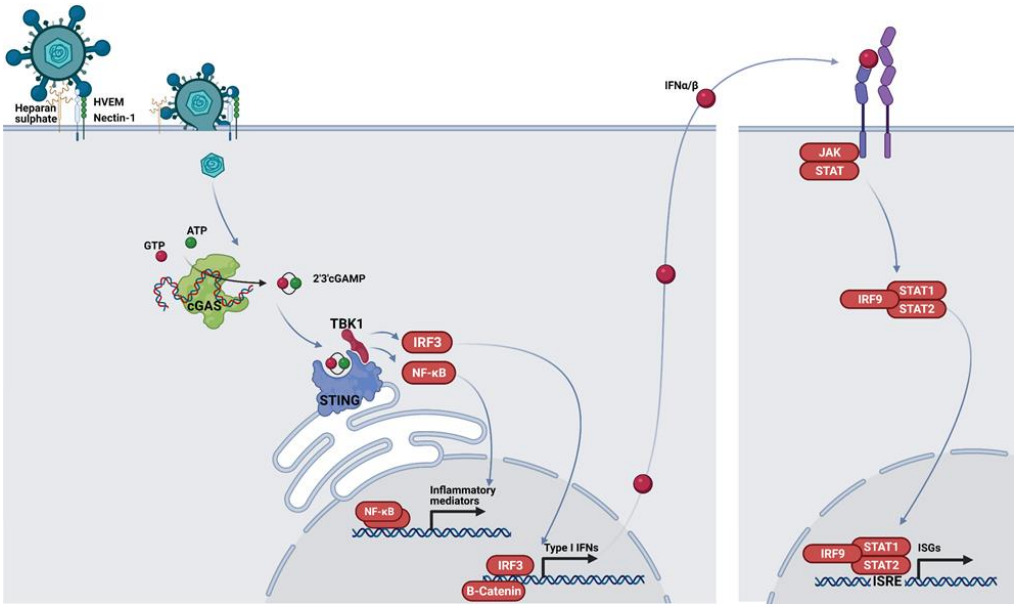

Figure 7. The cGAS-STING signalling pathway. The DNA sensor cGAS detects viral DNA and produces the second messenger 2'3'-cGAMP which binds to STING. Activated STING dimerizes and is ubiquitinated inducing a conformational change essential to anchor TBK1. This in turn triggers IRF3 activation and translocates into the nucleus inducing the expression of type I IFN. At the same time, activated STING induces NF-κB-dependent production of inflammatory mediators. IFNα/β in turns promote ISGs activation in bystander cells amplify the antiviral immune response.

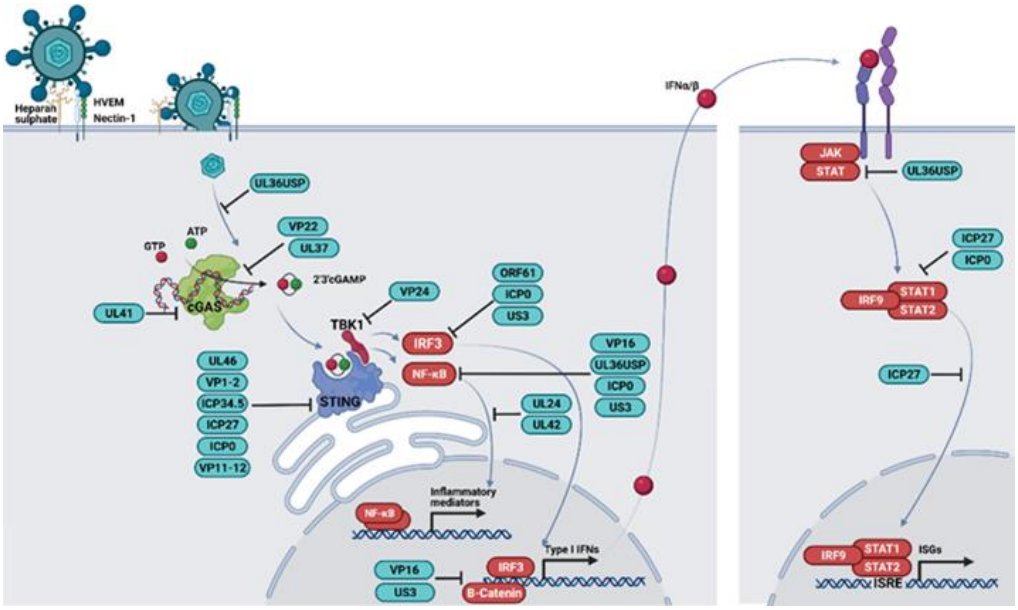

Figure 8. HSV-1 hampers STING signalling pathway. HSV-1 evolved a large number of mechanisms to hamper STING pathway at each step of its activation. The activity of cGAS-STING-TBK1-IRF3 is manipulated by the proteins shown in figure (light blue boxes).

3. Materials and Methods

3.1. Cell Culture, Manipulation and Characterization

LLC1-HER2 and LLC1-HER2_SKO were cultured in Dulbecco's Modified Eagle Medium (DMEM) supplemented with 2mM L-glutamine; SKOV3, CT26, CT26-HER2, CT26-HER2_SKO were cultured in RPMI 1640 Medium GlutaMAX™ Supplement. All media were supplemented with 10% FBS and Pen/Strep. Puromycin was used for human ERBB2 transgene stable expression. All the reagents were from Gibco™, Thermo Fisher Scientific Waltham, MA, USA. Cell lines were purchased from the American Type Culture Collection (ATCC) or kindly donated from collaborators and cultured in a humidified atmosphere containing 5% CO2 at 37 °C. To avoid *in vivo* immunogenicity of antibiotic resistant genes, Sting knockout was again carried out by CRISPR/Cas9 using pSpCas9(BB)-2A-GFP (PX458 ADDGENE, Watertown, MA, USA) with gRNA reported in Table 1. Knockout and functional rescue were assessed by Western blot. Filters were probed with the anti-STING antibody (Cell Signaling, Danvers, MA, USA, #13647), followed by anti-rabbit secondary antibody. Pierce™ ECL Western Blotting Substrate (Thermo Scientific, Waltham, MA, USA) was used for signal development, according to the manufacturer's recommendations. Human HER2 transduction of CT26 cells was performed by Origene, Rockville, MD, USA, RC212583L1V. To evaluate the HER2 expression, cells were stained with FITC-conjugated anti-human HER2 (ab31891 Abcam, Cambridge, UK) and analysed with FACS.

3.2. Cytotoxicity Assay

The lysis of virus-infected cells was determined by measuring the release of extracellular lactate dehydrogenase (LDH) from cells infected with R-LM113 at different MOI (1 pfu/cell and 5 pfu/10cell) over mock-infected cells by Pierce LDH Cytotoxicity Assay Kit (Thermo fisher Scientific, Waltham, MA, USA).

3.3. Virus Production, Titration and Real Time PCR Analysis

The R-LM113 virus used in this PhD project was described in Menotti et al. [49]. To titrate infectious viral particles, plaque assays were performed. Briefly, on day -1, 2.5E+05 SKOV3 cells were seeded in 12-well plates; at day 0, viral sample were diluted, from 1:10 to 1:10E + 09, in low serum RPMI medium in a final volume of 350 µL, and incubated with SKOV3 by gently shaking 90' at 37 °C. The media were replaced with 1 ml of low serum RPMI medium, and cells were cultured in a humidified atmosphere containing 5% CO2 at 37 °C. 120 hours later, cells were fixed with 100% ethanol for 10', stained with 10% GIEMSA for 15' and extensively washed with distilled water; plaques were counted to analyse infectious titre. To analyse the viral replication, genome copies were titrated by TaqMan RealTime PCR (Taqman universal PCR

mastermix, Applied Biosystems, Foster City, CA, USA) from cell lysates. Briefly, viral samples were diluted in A195 buffer and treated with RNase-free, DNase I recombinant enzyme (Roche, Basel, Switzerland) to remove envelope-free viral DNA. Enveloped viral DNA was thus extracted by SDS 0.1% (w/v, final concentration) and proteinase K (Roche, Basel, Switzerland). The extracted viral particles were diluted 1:10, 1:100 and 1:1000 and analysed by TaqMan RealTime PCR according to the manufacturer's recommendations (oligoes and probes in Table1).

3.4. *In Vivo* Studies and *Ex Vivo* Genome Copies Analysis

Female heterozygous B6.Cg-Pds5b<Tg(Wap-ERBB2)229Wzw>/J mice were used for *in vivo* studies. Mice were implanted subcutaneously on the right flank with 5×10^5 LLC1-HER2 or LLC1-HER2_SKO cells. Ten days after challenge, mice bearing established tumours were randomized according to tumour size, and 1E+08 viral PFU were injected intratumor in combination with intraperitoneally treatment with 200 µg α-mPD-1 (BioXcell, clone RMP114). The growth of tumours was measured by calliper every 3 or 4 days using the formula (LxW2)/2 [50]. Animals were sacrificed as soon as signs of distress or a tumour volume above 1500 mm3 occurred. *In vivo* viral replication was assessed 48 and 72 h after a single dose injection of 1E+08 viral PFU by TaqMan PCR. The experimental procedures were approved by the Italian Ministry of Health (Authorizations 213/2016 PR).

3.5. NanoString Data

Mice were implanted subcutaneously on the right flank with 5×10^5 LLC1-HER2 or LLC1-HER2_SKO cells. Ten days after challenge, mice bearing established tumours were randomized according to tumour size and treated with 1E+08 viral PFU intratumor injection or untreated. After 24 hours, the tumours were harvested, collected in RNA later (QIAGEN, Hilden, Germany) and stored at -80°. Tumours were lysed by Tissue Lyser LT (QIAGEN, Hilden, Germany) with 5 mm beads (QIAGEN, Hilden, Germany) in the presence of 2-mercaptoethanol (INVITROGEN, Carlsbad, CA, USA). To extract total RNA, an Rneasy Mini kit (QIAGEN, Hilden, Germany) was used. The extracted RNAs were analysed by nCounter Mouse PanCancer Immune Profiling Panel, in which were examined 770 immune-related genes, and Mouse PanCancer Pathways Panel, where we examined 770 genes belonging to 13 cancer-associated canonical pathways. Data were processed and normalized using nSolver Analysis Software.

3.6. *In Vitro* mRNA Dosage

IFN response-related genes were evaluated by using quantitative RT-PCR. Briefly, at day -1 LLC1-HER2, CT26-HER2, LLC-HER2_SKO and CT26-HER2_SKO cells were seeded in 12-well plates; at day 0 cells were transfected with 3 µg of interferon stimulatory DNA (ISD) (Invivogen, San Diego, CA, USA) in a ratio of 1:1 DNA/lipofectamine or with only lipofectamine 2000

(Invitrogen, Carlsbad, CA, USA). Ten hours after transfection, cells were lysed by TriFast (Euroclone, Pero, Italy) and total RNA was extracted with phenol/chloroform. Then, 3 µg of RNA was treated with RQ1 RNase-free DNase (Promega, Madison, WI, USA) to eliminate residual DNA contaminants. After Dnase inactivation for 10 min at 65 °C, 1 µg of RNA was reverse-transcribed by using ImProm-II Reverse Transcriptase (Promega, Madison, WI, USA) in a mix containing 3 mM MgCl2, 0.5mM dNTP and 500 ng random primer (Invitrogen, Carlsbad, CA, USA). The cDNA was then amplified in a 7500 Real-Time PCR System (Applied Biosystem, Foster City, CA, USA) using SYBR Green PCR Mastermix (Applied Biosystem, Foster City, CA, USA). All oligonucleotide primers were used to a final concentration of 0.2 µM (Table 1). The relative abundance of target RNAs was evaluated in relation to β-actin transcript by ΔΔCt method.

3.7. Immunogenic Cell Death

Immunogenic cell death mechanism was investigated through the extracellular release of ATP and High Mobility Group Box 1 (HMGB1). LLC1-HER2, CT26-HER2, LLC-HER2_SKO and CT26-HER2_SKO cells were seeded in 12-well plates and infected with R-LM113 at 1 and 10 pfu/cell or mock-infected. The supernatants were collected 24 h post infection and debris were removed by centrifugation at 200×g for 5 min. Secreted ATP was measured by ENLITEN ATP Assay System (Promega) according to the manufacturer's protocol. Supernatants were also used to detect HMGB1 with HMGB1 ELISA Kit (IBL International, Hamburg, Germany) following the manufacture's protocol outlined for the normal sensitivity format of the assay.

3.8. Statistical Analysis

GraphPad Prism was used to perform the following statistical analysis: Student's t-test, two-way ANOVA and Fisher's exact test. The significance was reported according to the following code $p < 0.05$ *; $p < 0.005$ **; $p < 0.0005$ ***; $p < 0.00005$ ****.

Table 1. Oligonucleotides.

Name	Oligonucleotide sequence
Taqman_DNApol_Fwd	5′-catcaccgacccggagagggac-3′
Taqman_DNApol_Rev	5′-gggccaggcgcttgttggtgta-3′
Taqman Probe	FAM-ccgccgaactgagcagacacccgcgc-Tamra
CCL5_RT_Fwd	5′-cctcaccatatggctcggac-3′
CCL5_RT_Rev	5′tcttctctgggttggcacac-3′
CXCL10_RT_ Fwd	5′-gccgtcattttctgcctcatc-3′
CXCL10_RT_ Rev	5′-taggctcgcagggatgatttc-3′
IFIT/ISG56_RT_Fwd	5′-tccgtaggaaacatcgcgtag-3′
IFIT/ISG56_RT_Rev	5′-tcttgcacattgtcctgcct-3′
IFNβ1_RT_Fwd	5′-atttctccagcactgggtgg-3′
IFNβ1_RT_Rev	5′-aggtacctttgcaccctcca-3′
CAS9_Fwd	5′-gctctttgatgccctcttcg-3′
CAS9_Rev	5′-gctgaccctgacactgtttg-3′
GFP_Fwd	5′-cacgacttcttcaagtccgc-3′
GFP_Rev	5′-ggtgttctgctggtagtggt-3′
GuideRNA_1	5′-gaggtcaccgctccaaatat-3′
GuideRNA_2	5′-cacctagcctcgcacgaact-3′
GuideRNA_3	5′-gggatgccccatccactgta-3′

4. Results

4.1. Setup of a Cellular System to Dissect Cancer Cell-Resident STING Pathway

Attenuated oncolytic HSV-1 widely infects different cell types (cancer, immune and stromal cells); thus, in order to study tumour-resident function of STING, I took advantage from the retargeted HSV-1 R-LM113. R-LM113 selectively infects cells expressing the human HER2 receptor, while it is de-targeted from the natural cellular ligands (HVEM, Nectin-1) due to the replacement of the viral glycoprotein D with a scFv targeting human HER2 [49]. This virus provides a useful tool to distinguish the function of the STING pathway within the tumour microenvironment. As preliminary characterizations, the expression of the key DNA sensing-mediating genes was analysed in both LLC1 and CT26 cell lines by RNA sequencing calculated as Transcripts Per Kilobase Million (TPM). As expected, in the absence of cytoplasmic DNA stimuli, the expression of type I IFNs gene resulted turned off in both cell lines (Figures 9 and 10). By DNA sequencing we verified the absence of inactivating mutation in cGAS and STING genes demonstrating the lack of biological bias (data not shown). Definitely, CT26 and LLC1 cell lines, respectively derived from BALB/c and C57BL/6 murine backgrounds, were selected as tumour models [50]. As preparatory to our study, murine CT26 and LLC1 cell lines were stably transduced with human HER2 cDNA to make them proficient for R-LM113 infection [51]. The correct display of human HER2 on the cell surfaces for both cell lines was confirmed by FACS analysis (Figure 11). Starting from HER2 knock-in cell lines, Sting KO clones were generated by CRISPR/Cas9 genome editing by guide RNA targeting the first and second coding exons of Sting (exons 3 and 4). For both cell lines, we identified Sting KO clones hereinafter referred as CT26-HER2_SKO and LLC1-HER2_SKO (Figure 12). Sting ablation was confirmed by Sanger sequencing, revealing the presence of indels and a premature occurrence of stop codon as result of non-homologous end joining DNA repair (data not shown). The absence of any residual protein expression was confirmed by Western Blot analysis confirming that all the Sting alleles were effectively targeted by Cas9 (Figure 13). To avoid an immunogenic response against any cloning residues (Cas9 and eGFP), the selected knock-out clones were screened by PCR to evidence potential integration of Cas9 and eGFP coding vectors (Figure 14). Finally, I compared the duplication rates of STING-KO cell lines to those of parental cells to ensure the absence of a different proliferation rate caused by Sting ablation (Figure 15).

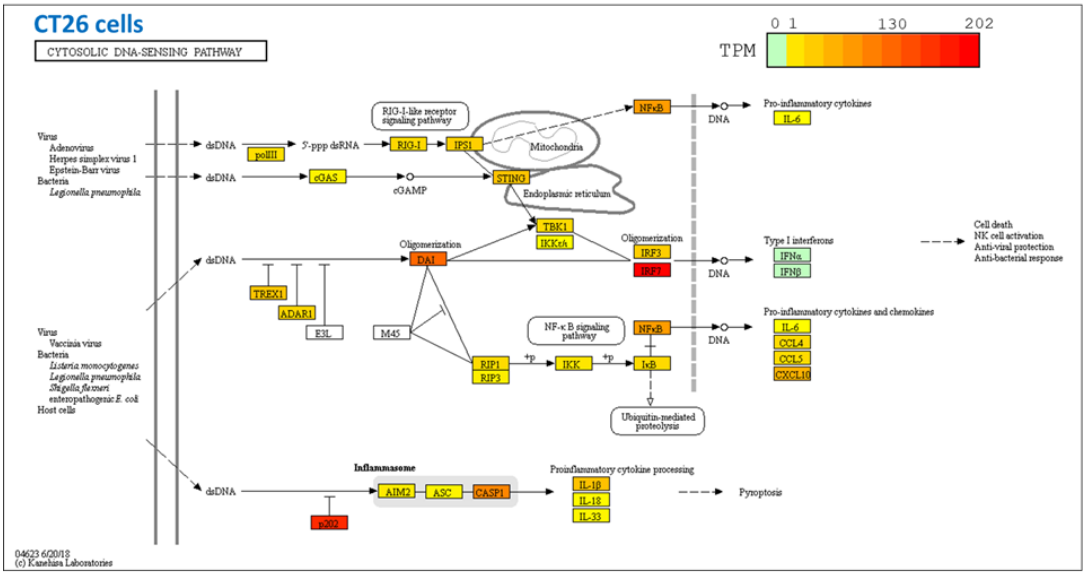

Figure 9. RNA sequencing analysis of genes involved in cytosolic DNA sensing in CT26 cell line. Mapping of genes involved in DNA sensing pathways was performed by using the Kegg mapper utility available in Kegg database. The abundance of transcripts was calculated by Transcripts Per Kilobase Million; the gradient of colours, shown in top right box from 202 to 0 TPM, correspond to the different grade of gene expression.

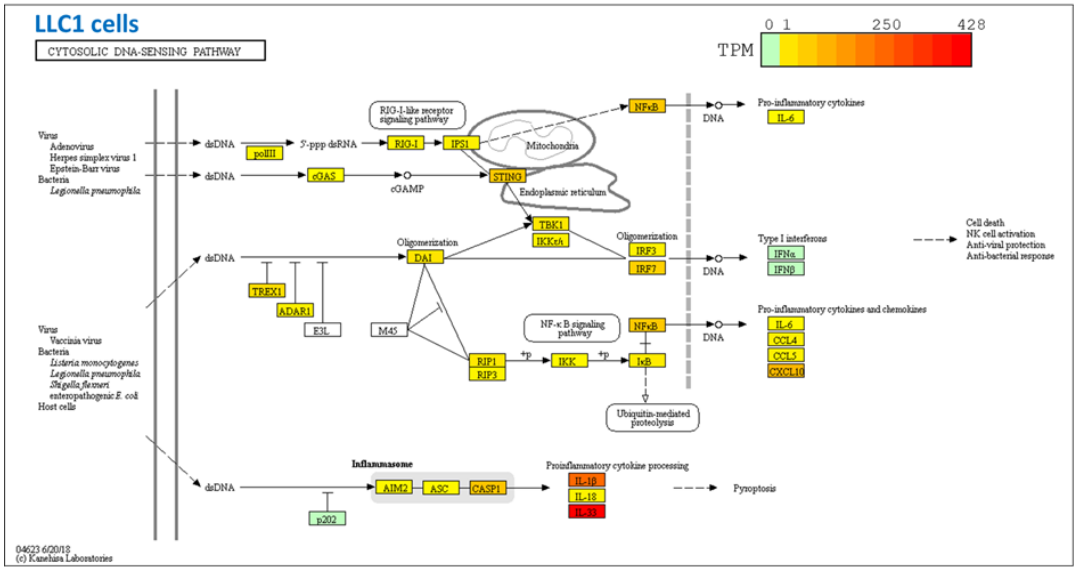

Figure 10. RNA sequencing analysis of genes involved in cytosolic DNA sensing in LLC1 cell line. *Mapping of genes involved in DNA sensing pathways was performed by using the Kegg mapper utility available in Kegg database. The abundance of transcripts was calculated by Transcripts Per Kilobase Million; the gradient of colours, shown in top right box from 428 to 0 TPM, correspond to the different grade of gene expression.*

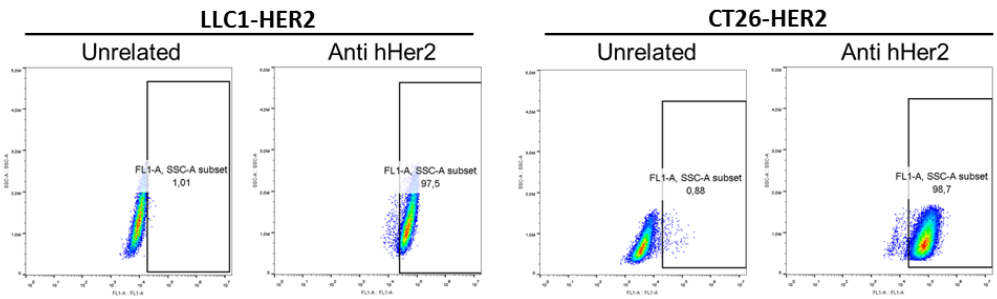

Figure 11. HER2 expression in murine LLC1 and CT26 cell lines. *Analysis of human HER2 display on cell surfaces of LLC1-HER2 (left) and CT26_HER2 (right) by FACS analysis; an unrelated antibody was used as negative control. LLC1-HER2 and CT26-HER2 cell lines show respectively 97,5% and 96,7% of positivity.*

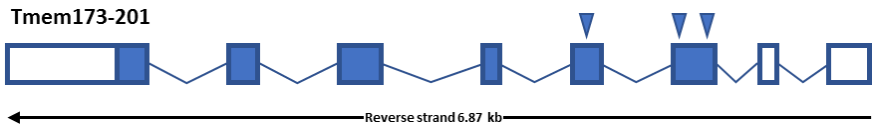

Figure 12. Cartoon of Tmem173 (transcript IDENSMUST00000115728.4) gene organization. Full and empty boxes respectively represent coding and untranslated exons. The positions of guide RNAs used for CRISPR/Cas9 genome editing to generate Sting knockout cancer cell lines are indicated by arrows.

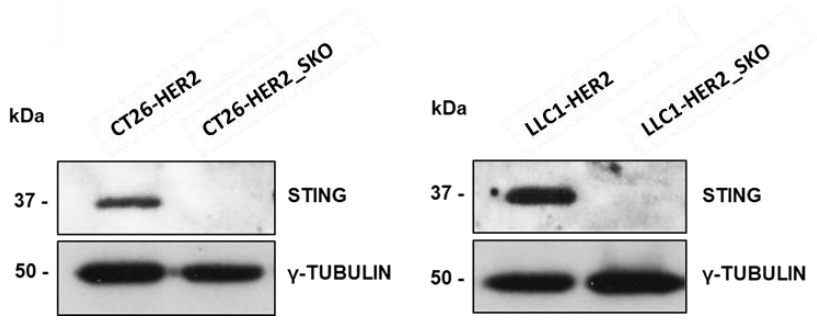

Figure 13. STING protein expression in KO cell lines. Western blot analysis of STING protein in CT26-HER2, LLC1-HER2 and their Sting knockout cell lines counterparts. Gamma tubulin detection was used for loading control.

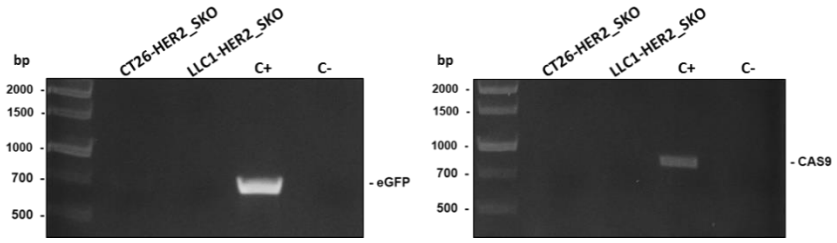

Figure 14. Evaluation of eGFP and Cas9 integration in HER2-SKO cell lines. PCR screening of CT26-HER2_SKO and LLC1_HER2_SKO cell lines to assess the absence of eGFP and Cas9 residues in genomic DNA. Cas9/eGFP-encoding vector was used as positive control (C+). Genomic DNA from parental CT26-HER2 and LLC-HER2 cell lines was used as negative control (C−).

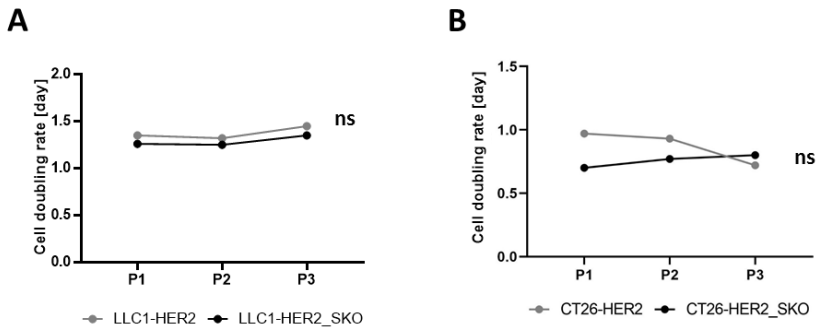

Figure 15. Evaluation of proliferation rate of Sting WT and SKO cell lines. Cell doubling per day were assessed for Sting wild-type (grey lines) and Sting knockout (black lines) LLC1 (A) and CT26 (B) cell lines. The differences in cell doubling were calculated by Student's t-test and were not statistically significant (ns) to each passage.

4.2. STING Restricts the Replicative Potential of HSV-1 in Cancer Cell Lines

To evaluate the impairment of Sting loss in tumour cells, I infected Sting KO and wild-type cells *in vitro* with the oncolytic R-LM113 virus. Both CT26-HER2_SKO and LLC1-HER2_SKO cell lines resulted more susceptible to oncolytic R-LM113, compared to their Sting wild-type counterparts. I evaluated the oncolytic virus spread, thanks to viral encoded eGFP expression, evidencing the formation of large lysis plaques in SKO cell lines compared to both parental cell lines (Figure 16). Thus, as expected, we confirmed that the increased viral replication was related to Sting absence. Interestingly, in accordance with previous reports in literature, a Sting knock down clone (presumably resulted from deletions in not all the alleles) showed an intermediate level of viral replication (Figures 17 and 18) [52-55]. I thus evaluated the lytic activity of R-LM113 through extracellular lactate dehydrogenase (LDH) release at different time points. According to viral spread, R-LM113 revealed a dose-dependent escalation in cytotoxicity in both CT26-HER2_SKO and LLC1-HER2_SKO cell lines compared to wild-type counterparts (Figure 19). I extended characterizations to viral genome replication and actual production of infectious viral particles. The inactivation of Sting exercised a disruptive gain in viral replication in both CT26-HER2_SKO and LLC1-HER2_SKO cell lines (Figure 20). In addition, it is to be noted the increasing of viral replication over time in Sting KO cell lines as opposed to the drop in viral replication in parental cells probably due to triggering of antiviral responses. These data were supported by a high increase in viral maturation and production for CT26-HER2_SKO and LLC1-HER2_SKO cell lines (Figure 21). Thus, the functional inactivation of Sting exerted gains in both viral replication and production, compared to the matching Sting wild-type cell lines, but the maturation of viral particles was particularly favoured by Sting inactivation (up to 250 times more). The obtained results support the relevant role of Sting in mediating cellular anti-viral responses, demonstrated in cell lines derived from two different genetic backgrounds. I replicated the same experiments with R-LM55 virus derived from wild-type strain F HSV-1. The increase in viral replication and production was confirmed in both CT26-HER2_SKO and LLC1-HER2_SKO cell lines revealing that an entry-independent mechanism is involved in the increased susceptibility of Sting-knockout cells to viral activities (Figures 22 and 23). To further prove that these biological effects were STING-dependent, I rescued STING function in CT26-HER2_SKO cells by transient transfection of a Sting-encoding vector (validated by WB analysis, Figure 24). The day after transfection, cells were infected with R-LM113 virus, and viral functions were monitored for up to 72 hours post infection. An empty vector was used as negative control. According to both viral spread and replication (in terms of genome copies and viral production), the antiviral activity was restored in tumour cells transfected with ectopic Sting, confirming its essential role (Figures 25 and 26). Based on aforementioned evidence, I

confirmed that, also in our models, Sting knock-out tumour cells are more susceptible to oncolytic viruses' infection, compared to Sting WT ones. It is to be noted that this OV model retains viral genes known to counteract Sting activity (i.e., γ34.5). This aspect further validates the key role of Sting [55-56]. Based on the collected data, it can be concluded that tumour cells with impaired DNA sensing Sting pathway could potentially represent an improved target for oncolytic virotherapy.

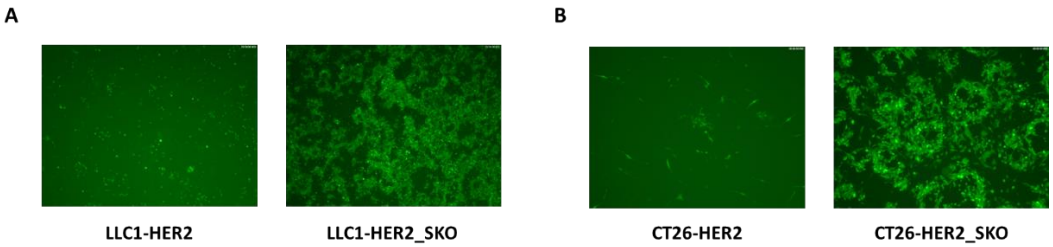

Figure 16. Comparison of viral spread in Sting knockout vs. parental wild-type cancer cell lines. Spread of eGFP-encoding R-LM113 was evaluated by fluorescence microscopy in STING wild-type and knockout LLC1 (A) and CT26 (B) cell lines.

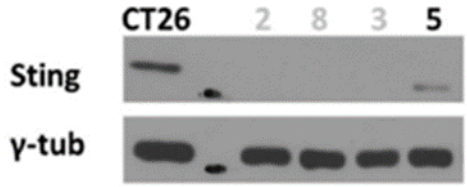

Figure 17. STING expression in knock down clones. The expression of Sting protein was evaluated by western blot analysis in different sub-clones. Clone n5 was selected as representative for knock down.

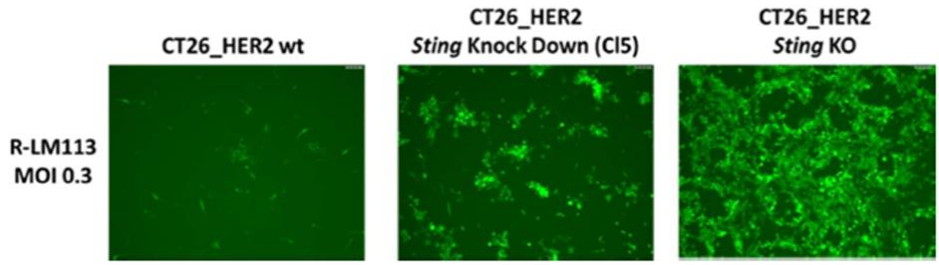

Figure 18. The knock down of Sting partially restores the replication of oncolytic R-LM113. Evaluation of viral spread in CT26_HER2 wild-type, Sting knock down and Sting KO cells by BAC encoded eGFP. Cells were infected at MOI 0.3 and spread efficiency was evaluated 72 h post infection.

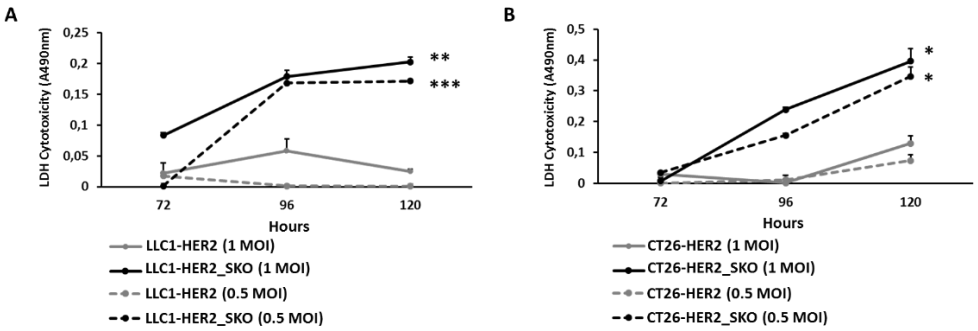

***Figure 19. Comparison of viral cytotoxicity in Sting knockout vs. parental wild-type cancer cell lines*.** (A) The lytic activity of R-LM113 was evaluated by extracellular LDH release in cell supernatants over the time course of infection (72, 96 and 120 h) in LLC1-HER2 (grey lines) and LLC1-HER2_SKO (black lines) at two different concentrations of viral particles (1 multiplicity of infection (MOI) continuous lines and 0.5 MOI dashed lines). (B) The same experiments performed in panel A were recapitulated in CT26-HER2 and CT26-HER2_SKO. All the infections were performed as biological replicates. The statistical significances for experiments described in panel A and B were calculated by Student's t-test comparing MOI-matched Sting wild-type vs. knockout cell lines. The p-values were 0.00115 and 0.000219, respectively, for 1 and 0.5 MOI in panel A; 0.01583, 0.008543, respectively, for 1 and 0.5 MOI in panel B.

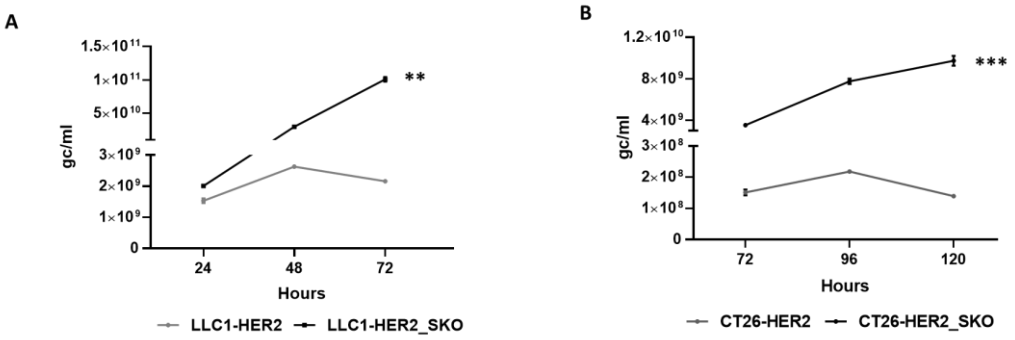

Figure 20. Evaluation of viral replication of R-LM113 in Sting wild-type and knockout cell lines. LLC1 (A) and CT26 (B) were infected with 0.3 PFU/cell R-LM113 virus. The qPCR-TaqMan analysis revealed the genome copies per mL (gc/mL) produced by the virus over time (24, 48, 72 h for LLC1 and 72, 96, 20 h for CT26). The statistical significances for experiments described in panel A and B were calculated by Student's t-test comparing Sting wild-type vs. knockout cell lines. The p-values calculated on biological replicates were 0.0013 for LLC1 cell line and 0.0005 for CT26 cell line.

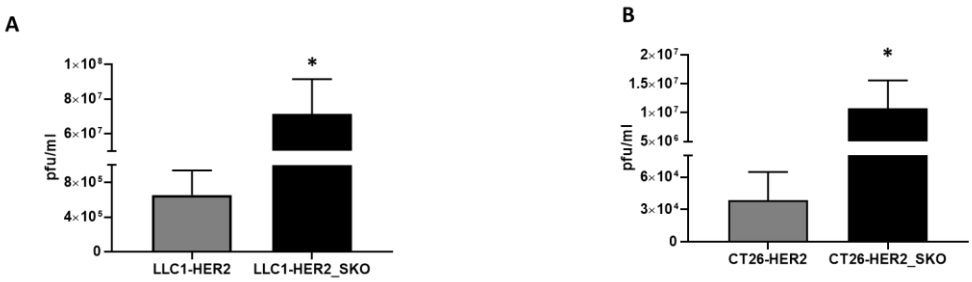

Figure 21. Analysis of the R-LM113 viral titres obtained in Sting wild-type and knockout LLC1 and CT26 cell lines. LL1 and CT26 were infected with 0.3 PFU/cell R-LM113 virus. Plaque assay was performed as biological replicate. The statistical significance for experiments described in panel A and B was calculated by Student's t-test comparing Sting wild-type vs. knockout cell lines. The p-values were 0.038 for LLC1 cell line and 0.02 for CT26 cell line. $p < 0.05$ *; $p < 0.005$ **; $p < 0.0005$ ***.

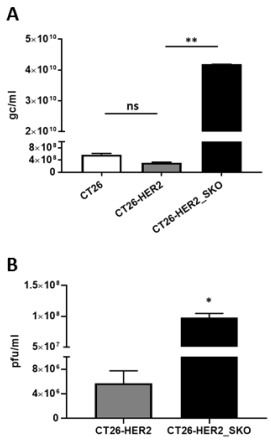

Figure 22. Comparison of viral effectiveness in CT26 Sting knockout vs parental wild-type cancer cell lines with R-LM55 virus. (A) Evaluation of viral replication of R-LM55 in CT26, CT26_HER2 and CT26_HER2_Sting knockout cell lines infected with 0.3 PFU/cell. The qPCR-TaqMan analysis revealed the genome copies per mL (gc/mL) produced by the virus at 96 hours post infection. The statistical significance was calculated by Student's t-test comparing Sting wild-type vs knockout cell lines, the P value resulted 0.0007. (B) Evaluation of the viral titres obtained in Sting wild-type and knockout CT26 cells with R-LM55 viruses (0.3 PFU/cell) by plaque assays at 96 hours post infection. The statistical significance was calculated by Student's t-test that resulted 0.03.

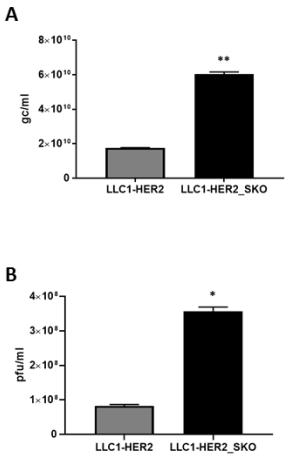

Figure 23. Comparison of viral effectiveness in LLC1 Sting knockout vs parental wild-type cancer cell lines with R-LM55 virus. The same experiments performed in figure 14 were replicated in LLC1-HER2 and LLC1-HER2_SKO. The statistical significance was calculated by Student's t-test that resulted respectively 0.0009 and 0.03 for panels A and B.

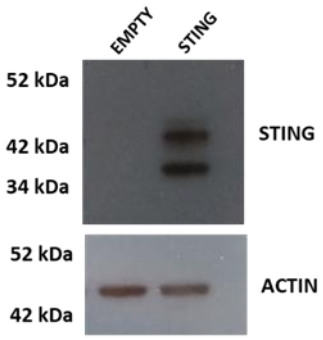

Figure 24. Functional rescue of STING in CT26-HER2_SKO cell line. CT26-HER2_SKO cell line were transiently transfected with a STING-encoding plasmid. Western Blot analysis of STING protein in mock and Sting-transfected CT26-HER2_SKO; ACTIN was used as standard.

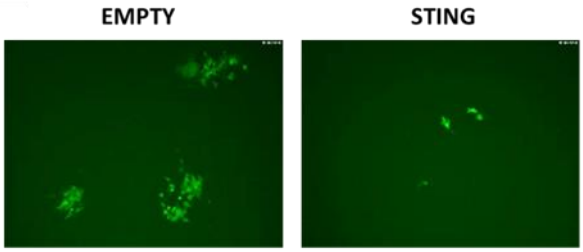

Figure 25. Functional rescue of STING in CT26-HER2_SKO cell line restored the resistance to oncolytic HSV-1. CT26-HER2_SKO cell line were transiently transfected with a STING-encoding plasmid and then infected with R-LM113 (0.1 PFU/cell). Evaluation of spread of eGFP-encoding R-LM113 in mock and Sting-transfected CT26-HER2_SKO cell line.

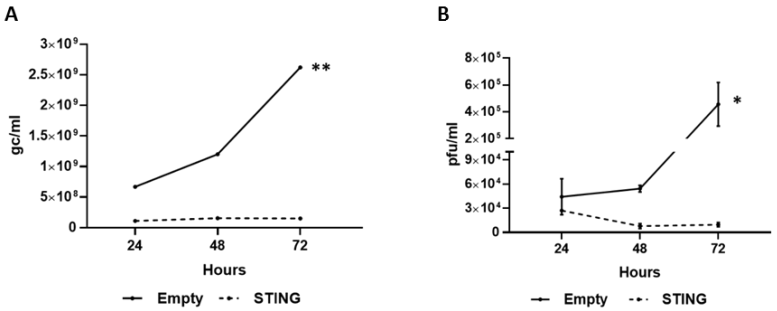

Figure 26. Functional rescue of STING in CT26-HER2_SKO cell line restored the resistance to oncolytic HSV-1. CT26-HER2_SKO cell line were transiently transfected with a STING-encoding plasmid and then infected with R-LM113 (0.1 PFU/cell). Evaluation of viral replication (A) and titre (B) of R-LM113 in mock and Sting-transfected CT26-HER2_SKO cell line. In panel A and B, gc and pfu per ml were calculated over time at indicated time points. The statistical significance was calculated by Student's t-test that resulted 0.0023 for viral replication, 0.05 for viral titre.

4.3. Sting_KO-dependent Improvements in Oncolytic Viral Replication and Cytotoxicity Do Not Correlate with Tumour Clearance Efficacy *In Vivo*

After having established that Sting-KO improves oHSV *in vitro* viral replication and cytotoxicity, I investigated the tumour-intrinsic Sting contribution *in vivo*. To explore the contribution of tumour-cell-intrinsic Sting to oncolytic efficacy, I used LLC1-syngeneic, human HER2-tolerant immunocompetent mouse model [51]. First, I investigated the viral replication in C57-HER2 tolerant mice that were injected subcutaneously with LLC1-HER2 or LLC1-HER2_SKO cells. After the tumours became established, *circa* 100 mm^3, mice were injected with a single intra-tumoral dose of R-LM113 virus (1E+08 PFU). The *in vivo* viral replication confirmed, similarly to the *in vitro* models, a sustained viral replication in Sting Knock-out tumours, compared to Sting wild-type (Figure 27). I thus assessed the antitumor efficacy of R-LM113 in LLC1-HER2 or LLC1-HER2_SKO tumour bearing mice. We and others previously reported that LLC1 tumour cell model is poorly responsive to immunotherapeutics including OVs and immune checkpoint inhibitors. For this reason, it is a very useful model to assess drug synergy. Accordingly, R-LM113 and PD-1 blockade administered as monotherapies were reported as ineffective in this model [57]. Thus, I tested the efficacy of R-LM113 in combination therapy with PD-1 immune checkpoint inhibition according to the treatment schedule reported in Figure 28 and previously reported as effective [36]. As reported in Figure 29, the engraftment rate and tumour growth of LLC1-HER2 and LLC1-HER2_SKO were almost identical. As expected for this tumour model, anti-PD1 blockade resulted ineffective as monotherapy (Figure 29). On the contrary, the combination therapy of oncolytic R-LM113 and anti PD-1 antibody in LLC1-HER2 cells resulted in 50% of complete response, since 4 out of 8 mice were tumour-free, in full agreement with our previous results (Figure 29) [36]. Surprisingly, mice bearing subcutaneous LLC1-HER2_SKO tumours resulted completely not responsive to combination therapy, as none of the treated mice resulted tumour-free by the end of the treatment (Figure 29). Interestingly, the tumour growth was delayed, compared to untreated group, probably due to the high lytic action of R-LM113 virus in Sting-deficient cells. Based on the aforementioned evidence, I speculated that the loss of Sting in tumour cells could be responsible for acquired resistance to onco-virotherapy. I thus investigated the molecular mechanisms responsible for these results. I hypothesized that the loss of Sting-dependent antiviral response might have hampered antitumor immunity. To address this hypothesis, a gene expression profiling was carried out through NanoString PanCancer Immune Profiling and PanCancer Mouse Pathway on tumour samples extracted from mock treated and virus-injected tumours of both wild-type and Sting knockout derivations. The wild-type treated tumours showed an overall upregulation in immune-related genes (Figure 30). In particular, I examined these differentially regulated genes according to STRING Gene Ontology (GO) showing that they cluster as anti-tumour immune

response signature. Among the most significant upregulated genes there are those involved in: T cell activation (Lat, Rorc), cytotoxic activity (Prf1, Gzma) and trafficking (Flna, Epha2); immune checkpoint modulators (Icos, Pd-l2, Ctla-4); innate immunity activators (Klrg1, Ccl19, Txk, Id2) (Figure 31). On the other hand, the Sting KO treated tumours were characterised by a down regulation of immune-related genes (Figure 32). According to GO they were classified in: PRRs (Rig-I, Zbp1, TLRs, Oas2, Oas3, Ifih1); IFN response; antigen presentation (MHCs, B2m); T cell function (TCR signalling, cytotoxicity, adhesion and migration, T helper cell function); NK cell function; cytokines, chemokines, and receptors (Figure 32). These genes cluster in cellular networks involved in antiviral response (in particular HSV response) (Figure 33). Instead, among the few upregulated genes in Sting KO treated tumours we identified: markers used to define resting cytotoxic T cells and predictor of short-term survivors (Lrrn3); oncogenes (Etv4); and Dusp4, recently described as a negative regulator of STING and RIG-I pathway cascade.

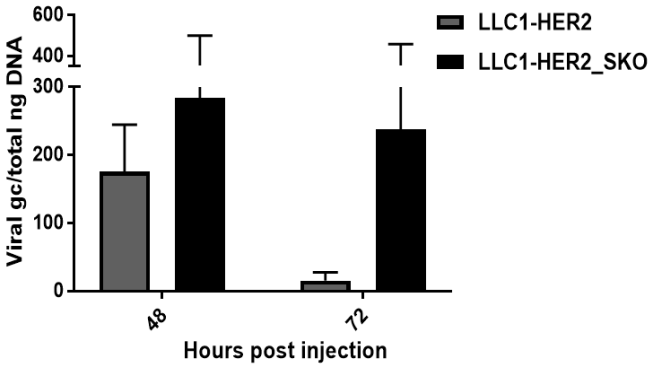

Figure 27. In vivo viral replication of oncolytic R-LM113 activity in vivo. Evaluation of *in vivo* intra-tumour viral replication in Sting wild-type and knockout LLC1 cell lines at 48 and 72 h after administration of R-LM113 (1E+08 viral PFU). Viral genome copies were quantified by TaqMan PCR and were normalized to total ng of extracted DNA. The statistical significance was calculated by two-way ANOVA (0.0148).

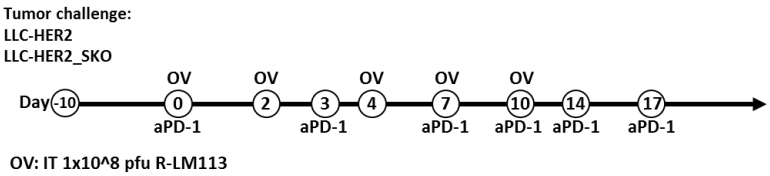

Figure 28. Schematic representation of the in vivo experimental setting. LLC1-HER2 wild-type and knockout cells were implanted subcutaneously into hHER2-transgenic/tolerant mice. When tumours became established (mean 110 mm3), mice were randomized according to tumour size. Mice received 5 intra-tumour injections of R-LM113 (1E+08 PFU/inj) at 0, 2, 4, 7, 10 days and six systemic administrations of PD-1 blocking antibody at days 0, 3, 7,10, 14, 17.

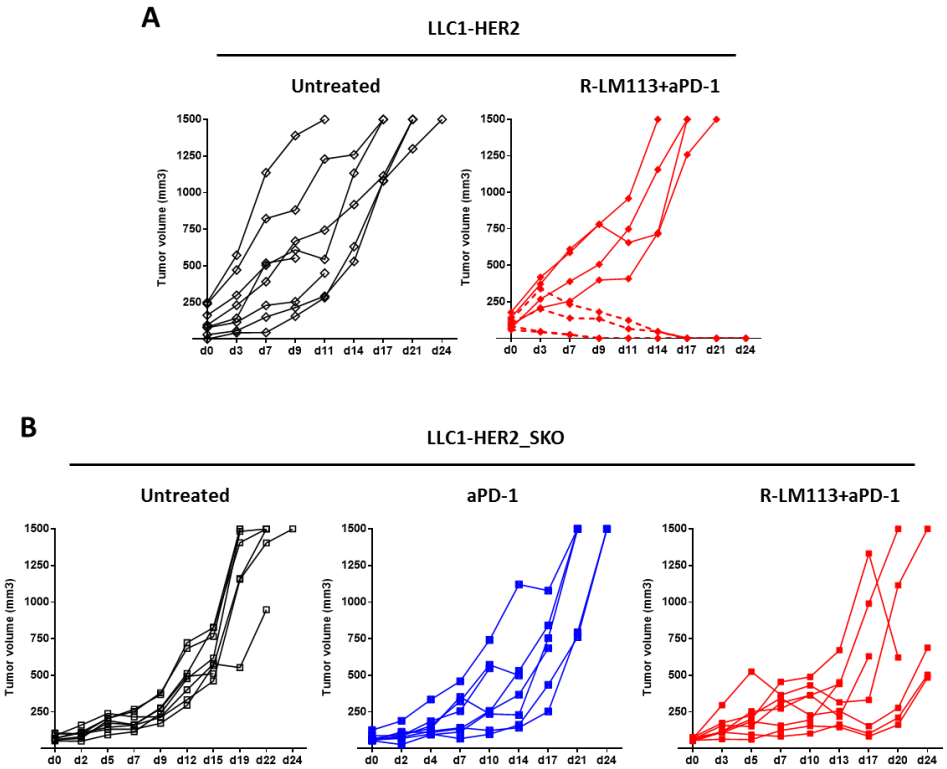

Figure 29. Tumour-resident STING influences oncolytic R-LM113 efficacy in vivo. (A) LLC-HER2 tumour growth in corresponding untreated (empty rhombuses) and combination treatment (red rhombuses). Dashed lines indicate complete responder mice. (B) LLC-HER2_SKO tumour growth for the three experimental groups: untreated (empty square), α-mPD-1 (blue) and combination (red square). For A and B, each line represents the tumour growth for individual mouse. The statistical significance for experiments described in panel A was calculated by Fisher's and was 0.03.

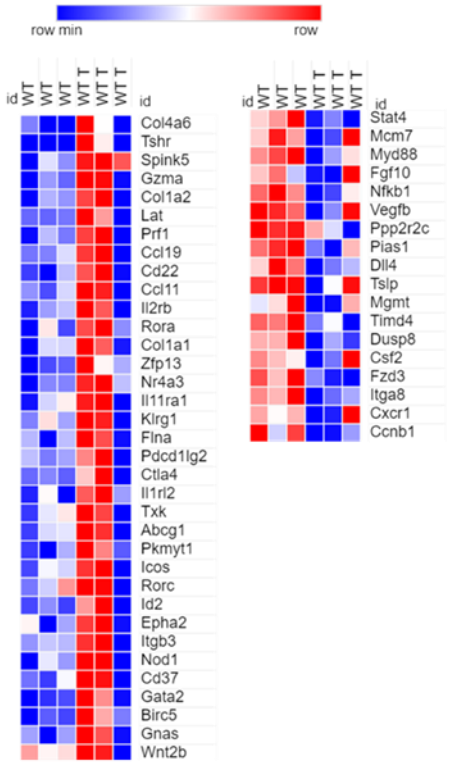

Figure 30. Gene expression profiling of Sting wild-type LLC1 tumours. A gene expression profiling was carried out for mock-treated and virus-injected Sting wild-type tumours. The image shown the full list of 54 differentially regulated genes as a heat map.

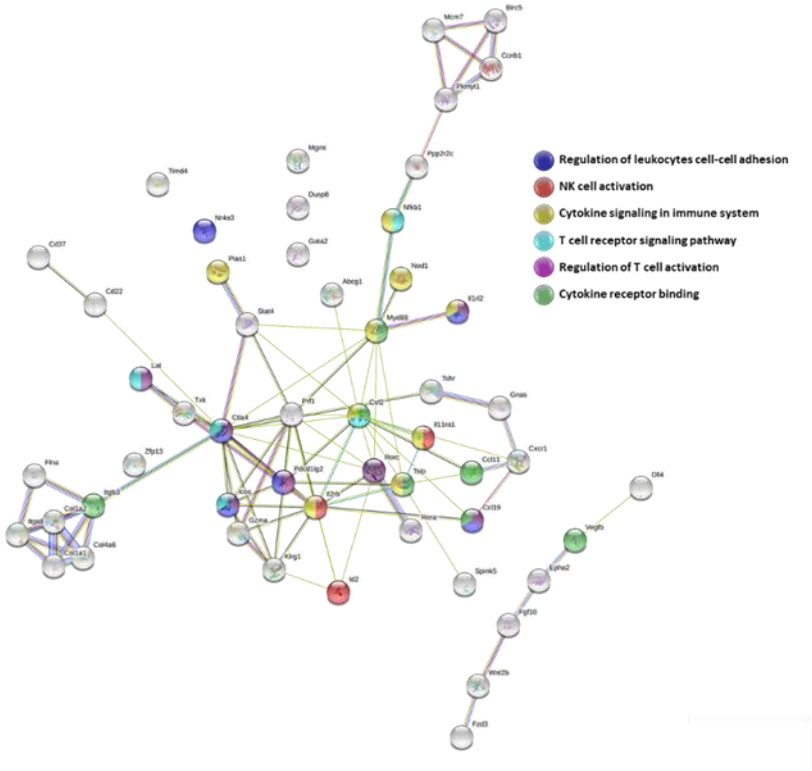

Figure 31. Gene expression profiling of Sting wild-type LLC1 tumours. A gene expression profiling was carried out for mock-treated and virus-injected Sting wild-type tumours. The image shown the full list of 54 differentially regulated genes as interaction networks processed by STRING software. The genes were labelled according to GO function reported in the picture.

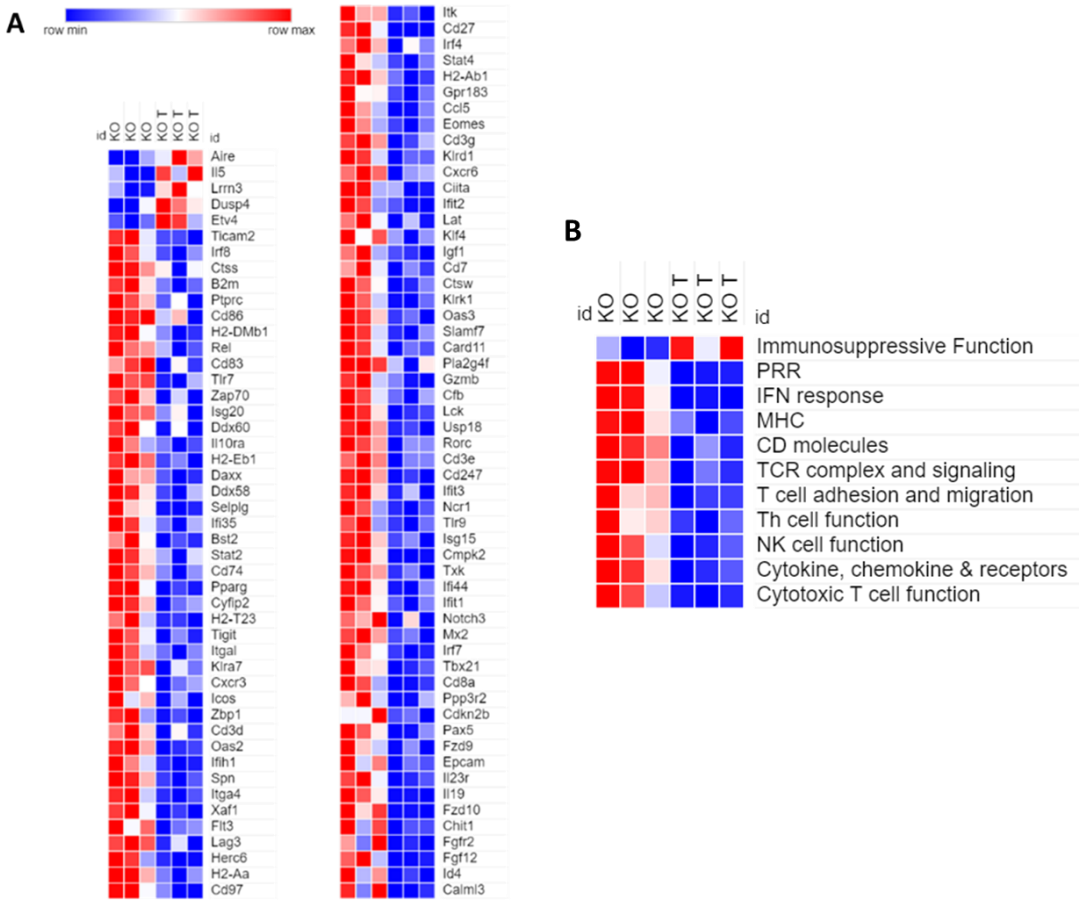

Figure 32. Gene expression profiling of Sting knockout LLC1 tumours. (A) A gene expression profiling was carried out for mock-treated and virus-injected Sting knockout tumours. The image shown the full list of differentially regulated genes as a heat map. (B) The genes were grouped in 11 immune relevant categories to obtain an overview of the gained trend from NanoString analysis.

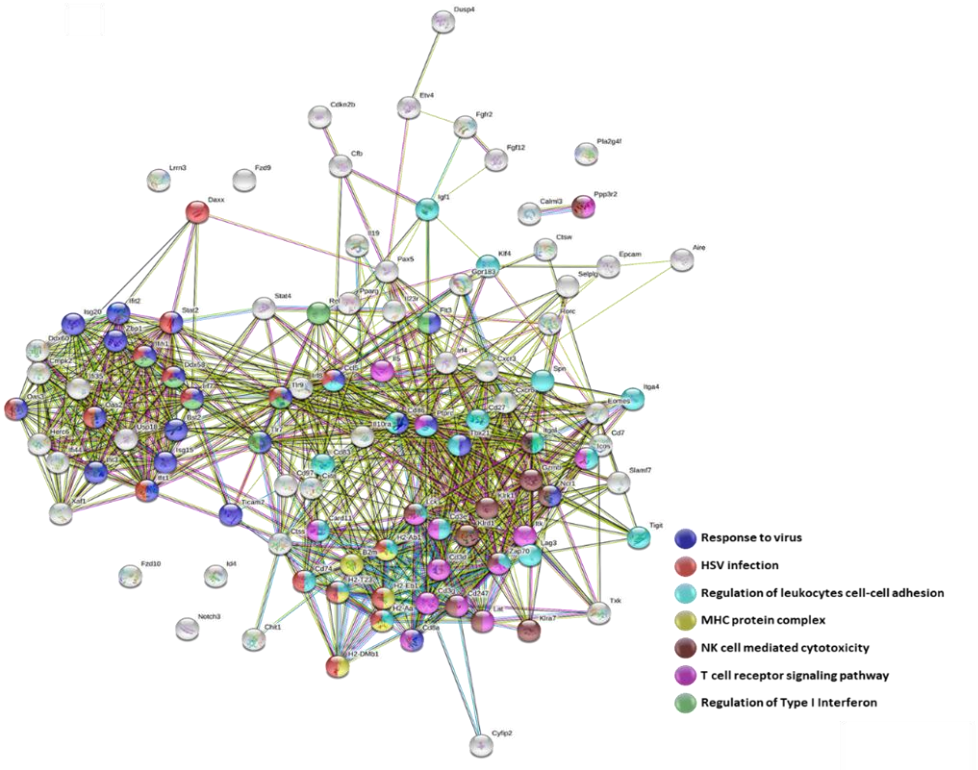

Figure 33. Gene expression profiling of Sting knock-out LLC1 tumours. A gene expression profiling was carried out for mock-treated and virus-injected Sting knock-out tumours. The image shown the full list of differentially regulated genes as interaction networks processed by STRING software. The genes were labelled according to GO function reported in the picture.

4.4. STING-deficient Tumour Cells Do Not Trigger Type I IFN Cascade and Show Impaired Immunogenic Cell Death Responses

Based on the described results, it can be speculated that the loss of Sting-dependent antiviral responses in tumour cells remodels the immunogenicity of tumour microenvironment. To investigate the molecular mechanisms responsible for these results, I explored two key events at the basis of antitumour activity exerted by oncolytic viruses: type I IFNs triggering and immunogenic cell death (ICD). I stimulated LLC-HER2 and LLC-HER2_SKO cell lines with interferon stimulatory DNA (ISD) to resemble Sting activation and I assessed the triggering of type I IFNs cascade pathway after 10 hours post treatment. In particular, I evaluated the expression of direct targets of Sting by RT-PCR, as well as the transcription of interferon stimulated genes (Ifn-β, CXCL10, CCL5, ISG56). In Sting knock-out cell line the transcription was dampened as result of loss of DNA sensing pathway. As expected, both Ifn-β and IFN-stimulated genes were upregulated after stimulus in Sting wild-type cell line (Figure 34). The same results were obtained with CT26 cell lines, underlining the central role of Sting in antiviral immunity (Figure 35).

To understand the Sting contribution to immunogenic cell death, I infected LLC-HER2 cell line and KO counterparts with R-LM113 at different MOIs (1 and 10). From the infected media, I measured the release of extracellular ATP and high-mobility group box 1 (HMGB1). Despite the relevant cell lysis assessed by LDH release (Figure 19), the infection failed to induce ICD in LLC-HER2 Sting knockout cell line. On the contrary, the infection mediated a dose-dependent ATP and HMGB1 release from Sting wild-type cells (Figure 36). To corroborate these results, I replicated the same experiment in the CT26 cellular background (Figure 37). These data shed light on Sting involvement in regulating immunogenicity of cell death, as its loss induced a more tolerogenic cell death, characterized by low release of immunogenic molecules (i.e., ATP, HMGB1), despite the consistent passive LDH release [58].

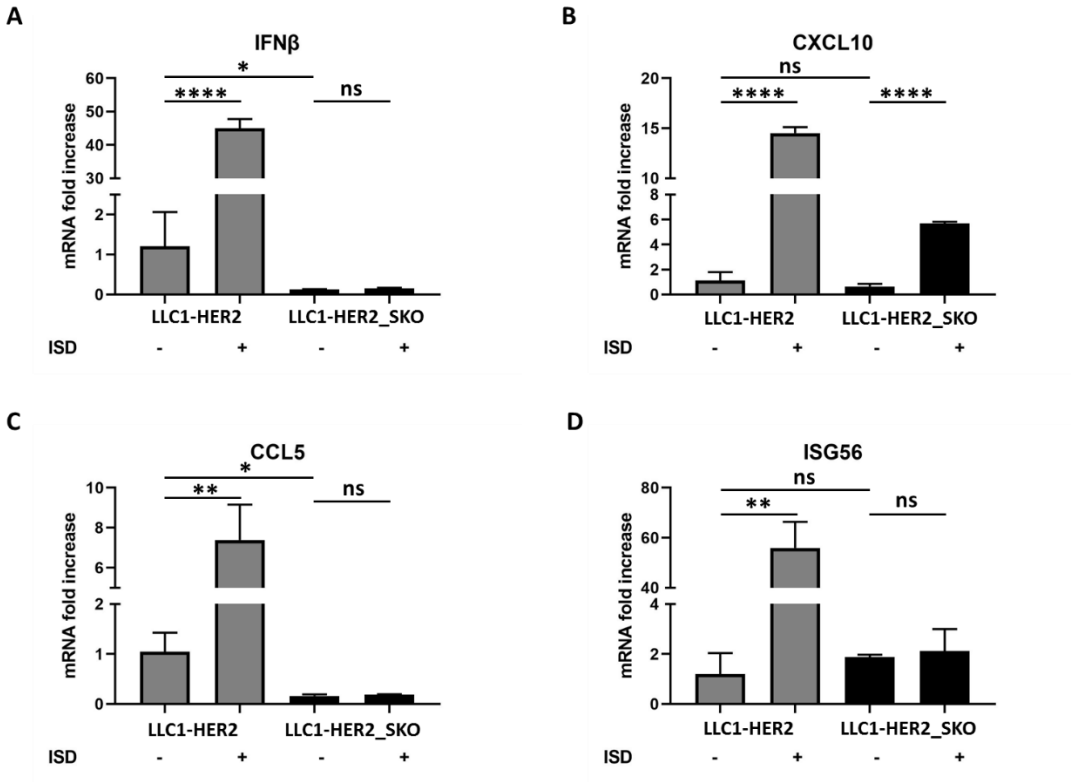

Figure 34. Induction of IFN-I cascade by DNA sensing in LLC1-HER2 Sting knockout and parental cancer cell lines. LLC1-HER2 cells and Sting knockout counterparts were stimulated in vitro by interferon stimulatory DNA (ISD). Ten hours post treatment, Ifnb (a), Cxcl10 (b), Ccl5 (c) and Isg56 (d) transcripts were assessed by real-time PCR. The relative abundance of target RNAs was evaluated in relation to Actinb transcript. The statistical significances for experiments described in Figure 34 were calculated by Student's t-test. Panel a, the p-values were 1.2E-5 comparing untreated and treated LLC1-HER2 and 0.01 comparing Sting wild-type vs. knockout cell lines. Panel b, the p-values were 1.2E-5 comparing untreated and treated LLC1-HER2 and 3E-6 comparing untreated and treated LLC1-HER2_SKO. Panel c, 0.003 comparing untreated and treated LLC1-HER2; 0.015 comparing Sting wild-type vs knockout cell lines. Panel d, 0.0008 comparing untreated and treated LLC1-HER2. Ns indicates statistically not significant differences calculated by Student's t-test. p <0.05 *; p <0.005 **; p <0.00005 ****.

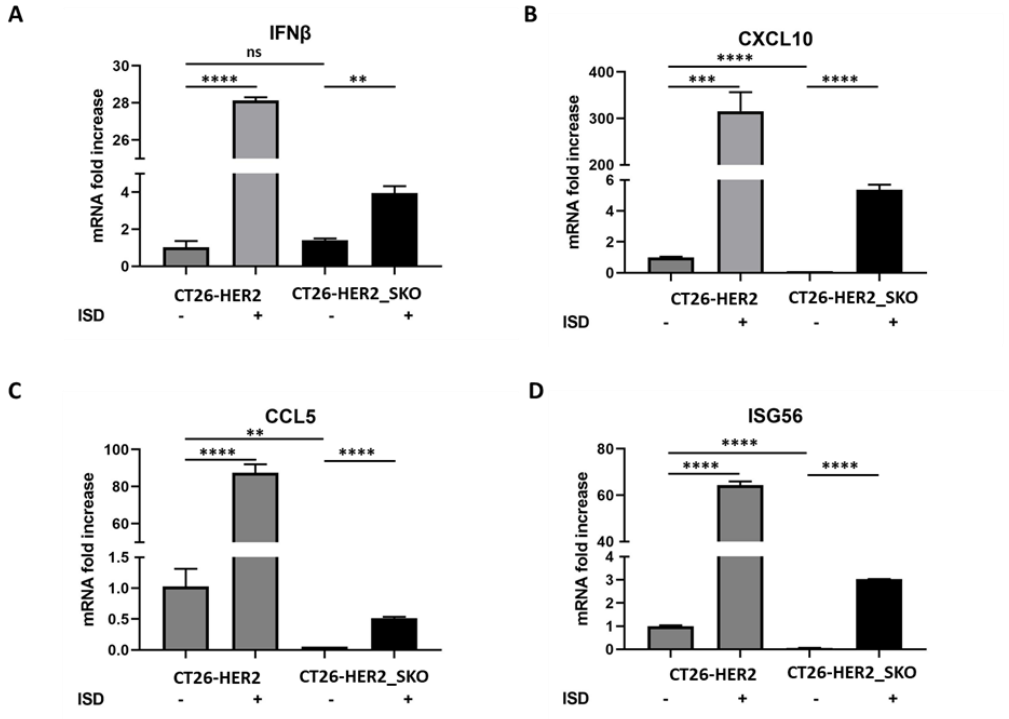

Figure 35. Induction of type-I IFN and related genes triggered by DNA sensing in CT26-HER2 Sting knockout and parental cancer cell lines. CT26-HER2 cells and Sting knockout counterpart were stimulated in vitro by ISD. Transcriptional activation of Ifnb (A), Cxcl10 (B), Ccl5 (C) and Isg56 (D) was assessed ten hours post treatment by Real time PCR. Actinb transcript was used to calculate the relative abundance of target genes. The statistical significances for experiments described in Figure 35 were calculated by Student's t-test. Ns indicates statistically not significant differences calculated by Student's t-test. p <0.005 **; p <0.0005 ***; p <0.00005 ****.

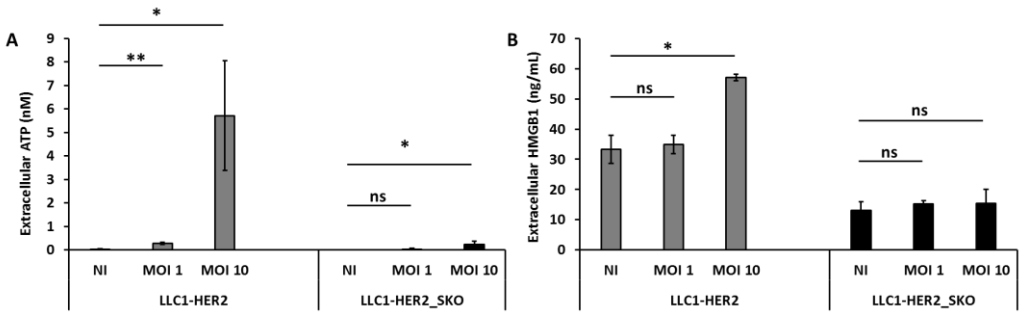

Figure 36. Sting expression in tumour cells is essential to induce oncolytic virus-mediated immunogenic cell death (LLC1 cell line). Evaluation of extracellular ATP (a) and HMGB1 (b) released in supernatant of mock or OV (oncolytic virus)-infected LLC1-HER2 and Sting knockout cells. Viral doses are indicated in each panel (1 and 10 PFU/cell). Infections were performed as biological replicates. The statistical significances for experiments described in Figure 36 were calculated by Student's t-test. Panel a, the p values were: 0.0008 comparing untreated and 1 MOI LLC1-HER2; 0.01 comparing untreated and 10 MOI LLC1-HER2_SKO. Panel b, the p-value was 0.0199 comparing untreated and 10 MOI LLC1-HER2. Ns indicates statistically not significant differences calculated by Student's t-test. $p < 0.05$ *; $p < 0.005$ **.

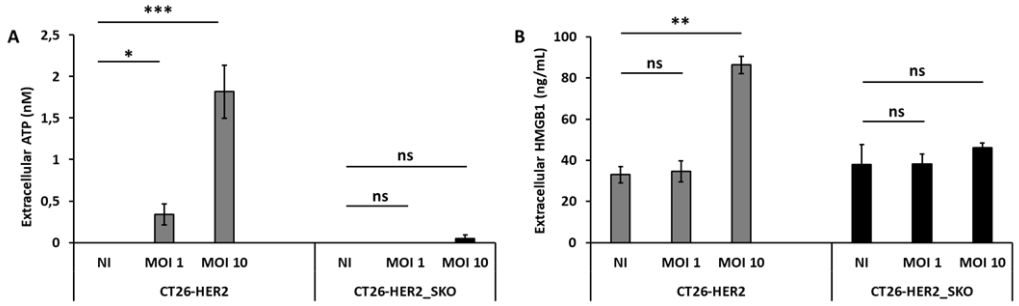

Figure 37. Sting expression in tumour cells is essential to induce oncolytic virus-mediated immunogenic cell death (CT26 cell line). Evaluation of extracellular ATP (a) and HMGB1 (b) released in supernatant of mock or OV (oncolytic virus)-infected CT26-HER2 and Sting knockout cells. Viral doses are indicated in each panel (1 and 10 PFU/cell). Infections were performed as biological replicates. The statistical significances for experiments described in Figure 37 were calculated by Student's t-test. Ns indicates statistically not significant differences calculated by Student's t-test. $p < 0.05$ *; $p < 0.005$ **; $p < 0.0005$ ***.

5. Discussion

Oncolytic viruses are a well-established class of immunotherapeutics for cancer treatments. After years of debate, the classical oncolytic-centric points of view, according to which "replication and lysis is everything", is overcome. Nowadays, a more immune-centric point of view has been widely accepted by the scientific community, in which the predominant contribution is mediated by immunogenic cell death [59]. Based on this mechanism of action, OVs can exert an immunolytic clearance of tumours by triggering an adaptive antitumour immune response. In the most extreme form of this point of view, OVs can be considered not so different from "old-school" antitumour adjuvant able to stimulate in a non-specific manner innate compartment of immune system as Toll-like receptor agonists. A clear example of this extreme concept has been shown by several groups implementing non-replicative oncolytic viruses (e.g., heat inactivated MVA) [60]. In a more balanced viewpoint, it is clear that the more viral replication happens in a tumour, greater is the triggering of immune stimulation. The immunotherapeutic potential of OVs is definitely demonstrated by abscopal antitumor efficacy, where OV-non-injected lesions also undergo regression upon boosting of tumour antigens-specific cytotoxic T lymphocytes [61]. These features contributed to define oncolytic viruses as agnostic cancer vaccines with a promising potential as synergistic agents in combination therapies with immune checkpoint modulators [62]. The efficacy of combination treatments depends on different factors including cancer immune profile, PD-1/PD-L1 expression and nature of cancer type [63]. In 2017, Liu *et al* demonstrated the improved therapeutic efficacy of oncolytic vaccinia virus and PD-L1 blockade. They showed how OV infection increases the migration of T cells in tumour site and induces PD-L1 expression in tumour and immune cells rendering the tumour more susceptible to anti-PD-L1 immunotherapy [64]. On the wave of these encouraging results, many other oncolytic viruses have been tested in combination with immune checkpoint inhibitors both in preclinical and clinical trials [65]. Although in early phase of the clinical trial (MASTERKEY-265), T-VEC plus Pembrolizumab (anti-PD-1), showed great results with 33% of complete response rate in 21 patients with advanced melanoma, the phase 3 did not meet the primary endpoints. Indeed, the difference in overall survival is minimal, as presented at recent Meetings of the European Society for Medical Oncology (ESMO) Congress 2021 and International Oncolytic Virus Conference (IOVC) congress 2021 [66-67]. We confirmed, in our experiments, the increases in *Pdcd1lg2* and *Ctla4* gene transcripts in STING WT tumours after oHSV infection assessed by Nanostring analysis, supporting the idea of a synergistic mechanism between immune checkpoint inhibitors and oncolytic viruses. Based on this evidence, there is a need to identify biomarkers responsible of immune-virotherapy resistance and predict in advance target patients that could take full advantage from onco-virotherapy.

In this context, adjuvant antitumour and innate antiviral effects are two sides of the same coin centred in PRRs. In detail, from a more "lytic" point of view, cGAS-STING signalling pathway is the

principal hurdle for replication of DNA-based oncolytic viruses, thus including HSV-1. On the other hand, from immune-centric view, activation of STING has been revealed as essential to elicit adaptive responses with agonist small molecules currently investigated in clinical trials as immunotherapeutics [68]. Based on this idea, we identified STING as a keystone to dissect oncolytic virus functions and the role of host innate antiviral immunity. As expected, experimental evidence already demonstrated the relationship between the loss of STING in tumour cells and the increase in OV-mediated cell lysis *in vitro* and in immunodeficient tumour-bearing mice [53-54, 69]. Based on such evidence, the idea that STING-KO tumours might be optimal targets for oncolytic virotherapy was proposed [54, 70]. A missing point to our knowledge is the clarification of immunotherapeutic STING functions in the framework of oncolytic therapy. Results obtained in my PhD project contributed to filling these gaps. Preclinical studies in tumour-bearing immunocompetent mice showed that the inactivation of tumour-intrinsic Sting, while favouring oncolytic viral replication, impairs the immunotherapeutic effect of combination therapy (oHSV-1 + α-PD1). In order to describe the molecular mechanisms underlying these phenomena, I analysed the transcriptomic profile of Sting KO *vs* Sting proficient tumours after injection of a tumour-targeted oncolytic herpes virus (R-LM113). While Sting proficient tumours rapidly exhibited a signature predictive for antitumour immune activation, Sting KO tumours resulted poorly immunogenic and generally repressed in immune functions. Immunogenic cell death was revealed as a main difference between Sting WT and KO tumours. Indeed, for the first time, a direct interplay between the Sting and ICD was demonstrated, where the loss of Sting corresponded to a dampened immunogenic cell death in response to onco-virotherapy. Accordingly, it can be proposed that antiviral, tumour-resident Sting provides fundamental contributions in heating-up the TME, eliciting immunotherapeutic efficacy of oncolytic viruses. Based on the evidence reported in this PhD project, I suppose that patients with loss-of-function in STING may not take full advantage from onco-virotherapy.

6. Appendix

This PhD thesis proposes a crucial role for cGAS-STING pathway in adjuvating OV-mediated antitumour immune response. Beyond acquired somatic loss-of-function mutations described in tumour tissues, several allelic variants and inherited mutations have been described in *STING* gene. Despite most of *STING* alleles are functional, several non-synonymous variants have been associated to disease conditions. Inherited gain-of-function mutations are mainly associated to *lupus*-like inflammatory syndrome, such as *STING*-associated Vasculopathy with onset in Infancy (SAVI) [71]. Looking at allelic variants, the most widespread ones are R232H and HAQ (R71H-G230A-R293Q) diffuse respectively in ~14% and ~20% of population [72]. Conflicting reports are present within the scientific literature, regarding the functionality of those *STING* variants. The reason why the functionality of these alleles has long evaded the understanding of scientists relies on the initial classification of H232 as reference allele. Among these, it was demonstrated that *STING* variants rescued in STING^{low} cells (293T) recognize differentially non-endogenous cyclic dinucleotides (e.g., bacterial c-di-GMP, c-di-AMP, 3'3'cGAMP), but all *STING* variants recognise the endogenous cGAS-synthetized 2'3'-cGAMP activating both IFN-b and NF-kB pathways [72]. In the same context, Jin et al. showed that, after stimulation by DNA plasmid, HAQ variant lost 90% of its activity, meanwhile R232H variant was comparable to WT (R232) for induction of IFN-β activity [73]. As opposite to Jin *et al.*, the Poland's lab showed decreased IFN cascade in 293T cells overexpressing R232H variant [74]. In hPBMCs from healthy volunteers, Ruiz-Moreno *et al.* showed a decreased IFN-β and TNF-α activity in HAQ genotype when stimulated by 2'3' cGAMP, while similar phenotype in R232H genotype [75-76]. In my opinion, the contradictory results emanating from these reports is due to the differential backgrounds of the experimental models. So, I decided to conduct a study on the actual contribution of the genetic variants in *STING*-mediated innate immune activation. To do this, I decided to exploit THP-1 cells, a human monocytic cell line derived from an acute monocytic leukaemia patient, able to differentiate in macrophages after stimulation. More in detail, I'm implementing THP-1 derivative cell lines stably expressing Luciferase and SEAP reporter genes under the control of IRF3 and TBK1 activities. On this homogeneous genetic background, I'm going to evaluate if there are differences in the four main STING alleles. The variants under investigations are: i. R232 as WT; ii. R232H; iii. HAQ; iv. V155M, used as a gain of function variant (SAVI). A STING-KO cell line is used as negative control. In a pilot experiment, I stimulated all the five cell lines with different stimuli (cyclic dinucleotides, DNA, RNA) and I evaluated IFN activation in time course analysis (18, 24 and 48 hours post stimulation) (Figure 38). As expected, all the cell lines equally responded to a STING-independent RNA stimulus (3p-hp-RNA). The suitability of the experimental system was further confirmed as: i. R232 cell line responded to DNA stimulus; ii. STING-KO cells didn't activate IFN pathway after STING-mediated stimuli (cGAMP, DNA); iii. M155 cell line activated downstream pathway, independently from stimuli. Surprisingly, IFN pathway was strongly

activated in THP-1 HAQ cell line by DNA and cGAMP stimuli, in a similar fashion to THP-1 bearing R232 allele. Moreover, R232H cells were impaired in triggering type I IFN pathway in response to both DNA and cGAMP. Currently, I'm investigating how these STING variants may actually respond to viral stimuli. This experimental model will be exploited to study the role of *STING* alleles as both: i. a risk factor for increased susceptibility to wild-type *Herpes* viruses in such population bearing given STING variants; ii. a potential predictive factor for clinical outcome to oncovirotherapy.

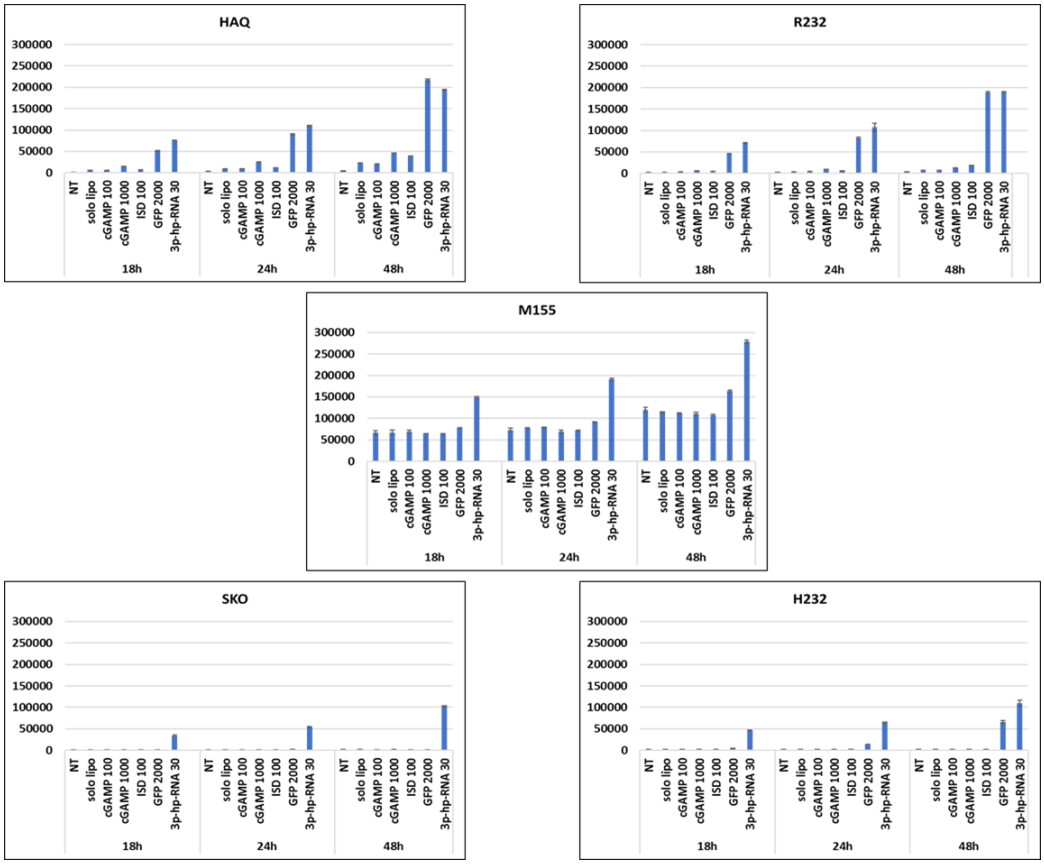

Figure 38. THP-1 STING variants have different IFN pathway activation. THP-1 HAQ cell line has a high activation after GFP stimulus and mild activation after cGAMP (1000ng/mL) and ISD stimuli.THP-1 cell line has a high activation after GFP stimulus. V155M cell line has a high activation in a stimuli-independent way. R232H cell line has a low activation only after GFP stimulus. All THP1 cell lines activate IFN pathway after RNA stimulus.

7. References

1. Oiseth SJ, Aziz MS. Cancer immunotherapy: a brief review of the history, possibilities, and challenges ahead. J Cancer Metastasis Treat 2017;3:250-61.

2. O'Donnell, J.S., Teng, M.W.L. & Smyth, M.J. Cancer immunoediting and resistance to T cell-based immunotherapy. Nat Rev Clin Oncol 16, 151–167 (2019). https://doi.org/10.1038/s41571-018-0142-8-.

3. Loeb L. A. (2011). Human cancers express mutator phenotypes: origin, consequences and targeting. Nature reviews. Cancer, 11(6), 450–457. https://doi.org/10.1038/nrc3063

4. Lindahl T, Wood RD. Quality control by DNA repair. Science 1999;286:1897-905.

5. Chen DS, Mellman I. Oncology meets immunology: the cancer-immunity cycle. Immunity. 2013 Jul 25;39(1):1-10. doi: 10.1016/j.immuni.2013.07.012. PMID: 23890059.

6. Dustin M. L. (2014). The immunological synapse. Cancer immunology research, 2(11), 1023–1033. https://doi.org/10.1158/2326-6066.CIR-14-0161

7. Qin, S., Xu, L., Yi, M. et al. Novel immune checkpoint targets: moving beyond PD-1 and CTLA-4. Mol Cancer 18, 155 (2019). https://doi.org/10.1186/s12943-019-1091-2.

8. Anderson AC, Joller N, Kuchroo VK. Lag-3, Tim-3, and TIGIT co-inhibitory receptors with specialized functions in immune regulation. Immunity.

9. Mascarelli DE, Rosa RSM, Toscaro JM, Semionatto IF, Ruas LP, Fogagnolo CT, Lima GC and Bajgelman MC (2021) Boosting Antitumor Response by Costimulatory Strategies Driven to 4-1BB and OX40 T-cell Receptors. Front. Cell Dev. Biol. 9:692982. doi: 10.3389/fcell.2021.692982

10. Ha D, Tanaka A, Kibayashi T, Tanemura A, Sugiyama D, Wing JB, Lim EL, Teng KWW, Adeegbe D, Newell EW, Katayama I, Nishikawa H, Sakaguchi S. Differential control of human Treg and effector T cells in tumor immunity by Fc-engineered anti-CTLA-4 antibody. Proc Natl Acad Sci U S A. 2019 Jan 8;116(2):609-618. doi: 10.1073/pnas.1812186116. Epub 2018 Dec 26. PMID: 30587582; PMCID: PMC6329979.

11. Park, J., Kwon, M. & Shin, EC. Immune checkpoint inhibitors for cancer treatment. Arch. Pharm. Res. 39, 1577–1587 (2016). https://doi.org/10.1007/s12272-016-0850-5.

12. Darvin, P., Toor, S.M., Sasidharan Nair, V. et al. Immune checkpoint inhibitors: recent progress and potential biomarkers. Exp Mol Med 50, 1–11 (2018).

13. Larkin J, Chiarion-Sileni V, Gonzalez R, Grob JJ, Cowey CL, Lao CD, et al. Combined nivolumab and ipilimumab or monotherapy in untreated melanoma. N Engl J Med. 2015;373:23–34. doi: 10.1056/NEJMoa1504030.

14. Robert, C. A decade of immune-checkpoint inhibitors in cancer therapy. Nat Commun 11, 3801 (2020). https://doi.org/10.1038/s41467-020-17670-y

15. Dempke WCM, Fenchel K, Uciechowski P, Dale SP. Second- and third-generation drugs for immuno-oncology treatment-The more the better? .Eur J Cancer. 2017 Mar;74:55-72. doi: 10.1016/j.ejca.2017.01.001. Epub 2017 Feb 10

16. Rosenberg SA, Restifo NP. Adoptive cell transfer as personalized immunotherapy for human cancer. Science. 2015 Apr 3;348(6230):62-8. doi: 10.1126/science.aaa4967

17. Guo, C., Manjili, M. H., Subjeck, J. R., Sarkar, D., Fisher, P. B., & Wang, X. Y. (2013). Therapeutic cancer vaccines: past, present, and future. Advances in cancer research, 119, 421–475. https://doi.org/10.1016/B978-0-12-407190-2.00007-1

18. Buonaguro L, Petrizzo A, Tornesello ML, Buonaguro FM. Translating tumor antigens into cancer vaccines. Clin Vaccine Immunol. 2011 Jan;18(1):23-34. doi: 10.1128/CVI.00286-10. Epub 2010 Nov 3. PMID: 21048000; PMCID: PMC3019775

19. O'Donnell JS, Teng MWL, Smyth MJ. Cancer immunoediting and resistance to T cell-based immunotherapy. Nat Rev Clin Oncol. 2019 Mar;16(3):151-167. doi: 10.1038/s41571-018-0142-8. PMID: 30523282.

20. Busch W. Aus der Sitzung der medicinischen Section vom 13 November 1867. Berlin Klin Wochenschr 1868;5:137. (in German)

21. Old LJ, Clarke DA, Benacerraf B. Effect of Bacillus Calmette-Guerin infection on transplanted tumours in the mouse. Nature 1959;184:291-2

22. Martuza RL, Malick A, Markert JM, Ruffner KL, Coen DM. Experimental therapy of human glioma by means of a genetically engineered virus mutant. Science. 1991;252:854–856.

23. Bischoff JR, Kirn DH, Williams A, et al. An adenovirus mutant that replicates selectively in p53-deficient human tumor cells. Science. 1996;274:373–376

24. Macedo N, Miller DM, Haq R, et al. Clinical landscape of oncolytic virus research in 2020. Journal for ImmunoTherapy of Cancer 2020;8:e001486. doi:10.1136/jitc-2020-001486

25. Bartlett, D.L., Liu, Z., Sathaiah, M. et al. Oncolytic viruses as therapeutic cancer vaccines. Mol Cancer 12, 103 (2013). https://doi.org/10.1186/1476-4598-12-103

26. Gujar S, Pol JG, Kim Y, Lee PW, Kroemer G. Antitumor Benefits of Antiviral Immunity: An Underappreciated Aspect of Oncolytic Virotherapies. Trends Immunol. 2018 Mar;39(3):209-221. doi: 10.1016/j.it.2017.11.006. Epub 2017 Dec 20. PMID: 29275092.

27. Sasso E, D'Alise AM, Zambrano N, Scarselli E, Folgori A, Nicosia A. New viral vectors for infectious diseases and cancer. Semin Immunol. 2020 Aug;50:101430. doi: 10.1016/j.smim.2020.101430. Epub 2020 Nov 29. PMID: 33262065.

28. Herpes Simplex Virus. Russell J. Diefenbach, Cornel Fraefel. 10.1007/978-1-4939-0428-0

29. Campadelli-Fiume G. Gianni T. HSV glycoproteins and their roles in virus entry and egress. In Alpha Herpesvirus Molecular and Cellular Biology 2006, Sandri-Goldin RM. Caister Academic Press: Norfolk, UK: 135-156

30. Campadelli-Fiume G., Amasio M., Avitabile E., Cerretani A., Forghieri C., Gianni T. and Menotti L. The multipartite system that mediates entry of herpes simplex virus into the cell. Medical. Virology. 2007; 17:313-326

31. Laquerre S., Argnani R., Anderson D.B., Zucchini S., Manservigi R. and Glorioso J.C. Heparan sulphate proteoglycan binding by herpes simplex virus type 1 glicoproteins B and C, which differ in their contributions to virus attachment, penetration, and cell-to-cell spread. Journal of Virology. 1998; 72:6119-6130.

32. Sanchala, D. S., Bhatt, L. K., & Prabhavalkar, K. S. (2017). Oncolytic Herpes Simplex Viral Therapy: A Stride toward Selective Targeting of Cancer Cells. Frontiers in pharmacology, 8, 270. https://doi.org/10.3389/fphar.2017.00270

33. Mohr I, Sternberg D, Ward S, Leib D, Mulvey M, Gluzman Y. A herpes simplex virus type 1 gamma34.5 second-site suppressor mutant that exhibits enhanced growth in cultured glioblastoma cells is severely attenuated in animals. J Virol. 2001 Jun;75(11):5189-96. doi: 10.1128/JVI.75.11.5189-5196.2001. PMID: 11333900; PMCID: PMC114924.

34. Kambara H, Okano H, Chiocca EA, Saeki Y. An oncolytic HSV-1 mutant expressing ICP34.5 under control of a nestin promoter increases survival of animals even when symptomatic from a brain tumor. Cancer Res. 2005 Apr 1;65(7):2832-9. DOI: 10.1158/0008-5472.CAN-04-3227

35. Zhang W, Ge K, Zhao Q, et al. A novel oHSV-1 targeting telomerase reverse transcriptase-positive cancer cells via tumor-specific promoters regulating the expression of ICP4. Oncotarget. 2015;6(24):20345-20355

36. Sasso E, Froechlich G, Cotugno G, D'Alise AM, Gentile C, Bignone V, De Lucia M, Petrovic B, Campadelli-Fiume G, Scarselli E, Nicosia A, Zambrano N. Replicative conditioning of Herpes simplex

type 1 virus by Survivin promoter, combined to ERBB2 retargeting, improves tumour cell-restricted oncolysis. Sci Rep. 2020 Mar 9;10(1):4307. doi: 10.1038/s41598-020-61275-w. PMID: 32152425; PMCID: PMC7062820.

37. Goins WF, Hall B, Cohen JB, Glorioso JC. Retargeting of herpes simplex virus (HSV) vectors.Curr Opin Virol. 2016 Dec;21:93-101. doi: 10.1016/j.coviro.2016.08.007. Epub 2016 Sep 8.

38. R Argnani, M Lufino, M Manservigi and R Manservigi. Replication-competent herpes simplex vectors: design and applications. Gene Therapy (2005) 12, S170–S177. doi:10.1038/sj.gt.3302622

39. Frampton AR Jr, Goins WF, Nakano K, Burton EA, Glorioso JC. HSV trafficking and development of gene therapy vectors with applications in the nervous system. Gene Ther. 2005 Jun;12(11):891-901.

40. Šedý JR, Spear PG, Ware CF. Cross-regulation between herpesviruses and the TNF superfamily members. Nature reviews Immunology. 2008;8(11):861-873. doi:10.1038/nri2434.

41. Campadelli-Fiume G, De Giovanni C, Gatta V, Nanni P, Lollini PL, Menotti L. Rethinking herpes simplex virus: the way to oncolytic agents. Rev Med Virol. 2011 Jul;21(4):213-26. doi: 10.1002/rmv.691. Epub 2011 May 27

42. Talimogene laherparepvec: review of its mechanism of action and clinical efficacy and safety

43. Osamu Takeuchi, Shizuo Akira, Pattern Recognition Receptors and Inflammation, Cell, Volume 140, Issue 6, 2010, Pages 805-820, ISSN 0092-8674, https://doi.org/10.1016/j.cell.2010.01.022.

44. Dambuza, I. M. & Brown, G. D. C-type lectins in immunity: recent developments. Curr. Opin. Immunol. 32, 21–27 (2015)

45. Goubau, D., Deddouche, S. & Reis e Sousa, C. Cytosolic sensing of viruses. Immunity 38, 855–869 (2013).

46. Chan YK, Gack MU. Viral evasion of intracellular DNA and RNA sensing. Nat Rev Microbiol. 2016 Jun;14(6):360-73. doi: 10.1038/nrmicro.2016.45. Epub 2016 May 13. PMID: 27174148; PMCID: PMC5072394.

47. Decout, A., Katz, J. D., Venkatraman, S., & Ablasser, A. (2021). The cGAS-STING pathway as a therapeutic target in inflammatory diseases. Nature reviews. Immunology, 21(9), 548–569. https://doi.org/10.1038/s41577-021-00524-z

48. Stempel M, Chan B, Brinkmann MM. Coevolution pays off: Herpesviruses have the license to escape the DNA sensing pathway. Med Microbiol Immunol. 2019 Aug;208(3-4):495-512. doi: 10.1007/s00430-019-00582-0. Epub 2019 Feb 25. PMID: 30805724.

49. Menotti, L.; Cerretani, A.; Hengel, H.; Campadelli-Fiume, G. Construction of a Fully Retargeted Herpes Simplex Virus 1 Recombinant Capable of Entering Cells Solely via Human Epidermal Growth Factor Receptor 2. J. Virol. 2008, 82, 10153–10161, doi:10.1128/jvi.01133-08.

50. Lechner, M.G.; Karimi, S.S.; Barry-Holson, K.; Angell, T.E.; Murphy, K.A.; Church, C.H.; Ohlfest, J.R.; Hu, P.; Epstein, A.L. Immunogenicity of Murine Solid Tumor Models as a Defining Feature of In Vivo Behavior and Response to Immunotherapy. J. Immunother. 2013, 36, 477–489, doi:10.1097/01.cji.0000436722.46675.4a

51. Leoni, V.; Vannini, A.; Gatta, V.; Rambaldi, J.; Sanapo, M.; Barboni, C.; Zaghini, A.; Nanni, P.; Lollini, P.-L.; Casiraghi, C.; et al. A Fully-Virulent Retargeted Oncolytic HSV Armed with IL-12 Elicits Local Immunity and Vaccine Therapy Towards Distant Tumors. PLoS Pathog. 2018, 14, e1007209, doi:10.1371/journal.ppat.1007209

52. Konno, H.; Yamauchi, S.; Berglund, A.; Putney, R.M.; Mulé, J.J.; Barber, G.N. Suppression of STING Signaling through Epigenetic Silencing and Missense Mutation Impedes DNA Damage Mediated Cytokine Production. Oncogene 2018, 37, 2037–2051, doi:10.1038/s41388-017-0120-0.

53. Xia, T.; Konno, H.; Barber, G.N. Recurrent Loss of STING Signaling in Melanoma Correlates with Susceptibility to Viral Oncolysis. Cancer Res. 2016, 76, 6747–6759, doi:10.1158/0008-5472.can-16-1404.

54. De Queiroz, N.M.G.P.; Xia, T.; Konno, H.; Barber, G.N. Ovarian Cancer Cells Commonly Exhibit Defective STING Signaling Which Affects Sensitivity to Viral Oncolysis. Mol. Cancer Res. 2018, 17, 974–986, doi:10.1158/1541-7786.mcr-18-0504.

55. Lee, J.M.; Ghonime, M.G.; Cassady, K.A. STING Restricts OHSV Replication and Spread in Resistant MPNSTs but Is Dispensable for Basal IFN-Stimulated Gene Upregulation. Mol. Ther. Oncolytics 2019, 15, 91–100, doi:10.1016/j.omto.2019.09.001.

56. Pan, S.; Liu, X.; Ma, Y.; Cao, Y.; He, B. Herpes Simplex Virus 1 γ134.5 Protein Inhibits STING Activation That Restricts Viral Replication. J. Virol. 2018, 92, e01015-18, doi:10.1128/jvi.01015-18.

57. De Lucia, M.; Cotugno, G.; Bignone, V.; Garzia, I.; Nocchi, L.; Langone, F.; Petrovic, B.; Sasso, E.; Pepe, S.; Froechlich, G.; et al. Retargeted and Multi-Cytokine Armed Herpes Virus is a Potent Cancer Endovaccine for Local and Systemic Anti-Tumor Treatment in Combination with Anti-PD1. Mol. Ther. Oncolytics 2020, doi:10.1016/j.omto.2020.10.006

58. Michaud, M.; Xie, X.; Pedro, J.M.B.-S.; Zitvogel, L.; White, E.; Kroemer, G. An Autophagy-Dependent Anticancer Immune Response Determines the Efficacy of Melanoma Chemotherapy. OncoImmunology 2014, 3, e944047, doi:10.4161/21624011.2014.944047.

59. Vile, R.G. The Immune System in Oncolytic Immunovirotherapy: Gospel, Schism and Heresy. Mol. Ther. 2018, 26, 942–946, doi:10.1016/j.ymthe.2018.03.007

60. Dai P, Wang W, Yang N, Serna-Tamayo C, Ricca JM, Zamarin D, Shuman S, Merghoub T, Wolchok JD, Deng L. Intratumoral delivery of inactivated modified vaccinia virus Ankara (iMVA) induces systemic antitumor immunity via STING and Batf3-dependent dendritic cells. Sci Immunol. 2017 May 19;2(11):eaal1713. doi: 10.1126/sciimmunol.aal1713. PMID: 28763795; PMCID: PMC5559204

61. Russell SJ, Barber GN. Oncolytic Viruses as Antigen-Agnostic Cancer Vaccines. Cancer Cell. 2018 Apr 9;33(4):599-605. doi: 10.1016/j.ccell.2018.03.011. PMID: 29634947; PMCID: PMC5918693.

62. Chesney, J.; Puzanov, I.; Collichio, F.; Singh, P.; Milhem, M.M.; Glaspy, J.; Hamid, O.; Ross, M.; Friedlander, P.; Garbe, C.; et al. Randomized, Open-Label Phase II Study Evaluating the Efficacy and Safety of Talimogene Laherparepvec in Combination With Ipilimumab Versus Ipilimumab Alone in Patients with Advanced, Unresectable Melanoma. J. Clin. Oncol. 2018, 36, 1658–1667, doi:10.1200/jco.2017.73.7379.

63. Brian A. Jonas. Combination of an oncolytic virus with PD-L1 blockade keeps cancer in check. Science Translational Medicine. Vol. 9, Issue 386. DOI: 10.1126/scitranslmed.aan2781

64. Liu, Z., Ravindranathan, R., Kalinski, P. et al. Rational combination of oncolytic vaccinia virus and PD-L1 blockade works synergistically to enhance therapeutic efficacy. Nat Commun 8, 14754 (2017). https://doi.org/10.1038/ncomms14754

65. Sivanandam, V., LaRocca, C. J., Chen, N. G., Fong, Y., & Warner, S. G. (2019). Oncolytic Viruses and Immune Checkpoint Inhibition: The Best of Both Worlds. Molecular therapy oncolytics, 13, 93–106. https://doi.org/10.1016/j.omto.2019.04.003

66. Ribas A, Chesney J, Long GV, et al. MASTERKEY-265: A phase III, randomized, placebo-controlled study of talimogene laherparepvec plus pembrolizumab for unresectable stage III-IVM1c melanoma. Presented at: European Society for Medical Oncology (ESMO) Congress 2021; September 16-21, 2021. Abstract 1037O

67. Gogas H. Amgen Phase 3 T-Vec Melanoma Trial. International Oncolytic Virus Conference (IOVC) Congress 2021.

68. Davola, M.E.; Mossman, K.L. Oncolytic Viruses: How “Lytic” Must They be for Therapeutic Efficacy? Oncoimmunology 2019, 8, e1581528.

69. Xia T, Konno H, Ahn J, Barber GN. Deregulation of STING Signaling in Colorectal Carcinoma Constrains DNA Damage Responses and Correlates With Tumorigenesis. Cell Rep. 2015;14(2):282–297. doi:10.1016/j.celrep.2015.12.029

70. Tumor-Derived cGAMP Triggers a STING-Mediated Interferon Response in Non-tumor Cells to Activate the NK Cell Response, Assaf Marcus, Amy J. Mao, Monisha Lensink-Vasan, LeeAnn Wang, Russell E. Vance, David H. Raulet, Show footnotes, Published: October 16, 2018, DOI:https://doi.org/10.1016/j.immuni.2018.09.016

71. Jeremiah N, Neven B, Gentili M, Callebaut I, Maschalidi S, Stolzenberg MC, Goudin N, Frémond ML, Nitschke P, Molina TJ, Blanche S, Picard C, Rice GI, Crow YJ, Manel N, Fischer A, Bader-Meunier B, Rieux-Laucat F. Inherited STING-activating mutation underlies a familial inflammatory syndrome with lupus-like manifestations. J Clin Invest. 2014 Dec;124(12):5516-20. doi: 10.1172/JCI79100. Epub 2014 Nov 17. PMID: 25401470; PMCID: PMC4348945.

72. Yi G, Brendel VP, Shu C, Li P, Palanathan S, Cheng Kao C. Single nucleotide polymorphisms of human STING can affect innate immune response to cyclic dinucleotides. PLoS One. 2013 Oct 21;8(10):e77846. doi: 10.1371/journal.pone.0077846. PMID: 24204993; PMCID: PMC3804601.

73. Jin L, Xu LG, Yang IV, Davidson EJ, Schwartz DA, Wurfel MM, Cambier JC. Identification and characterization of a loss-of-function human MPYS variant. Genes Immun. 2011 Jun;12(4):263-9. doi: 10.1038/gene.2010.75. Epub 2011 Jan 20. PMID: 21248775; PMCID: PMC3107388.

74. Kennedy RB, Haralambieva IH, Ovsyannikova IG, Voigt EA, Larrabee BR, Schaid DJ, Zimmermann MT, Oberg AL, Poland GA. Polymorphisms in STING Affect Human Innate Immune Responses to Poxviruses. Front Immunol. 2020 Oct 14;11:567348. doi: 10.3389/fimmu.2020.567348. PMID: 33154747; PMCID: PMC7591719.

75. Ruiz-Moreno JS, Hamann L, Shah JA, Verbon A, Mockenhaupt FP, Puzianowska-Kuznicka M, Naujoks J, Sander LE, Witzenrath M, Cambier JC, Suttorp N, Schumann RR, Jin L, Hawn TR, Opitz B; CAPNETZ Study Group. The common HAQ STING variant impairs cGAS-dependent antibacterial responses and is associated with susceptibility to Legionnaires' disease in humans. PLoS Pathog. 2018 Jan 3;14(1):e1006829. doi: 10.1371/journal.ppat.1006829. PMID: 29298342; PMCID: PMC5770077

76. Patel S, Blaauboer SM, Tucker HR, Mansouri S, Ruiz-Moreno JS, Hamann L, Schumann RR, Opitz B, Jin L. The Common R71H-G230A-R293Q Human TMEM173 Is a Null Allele. J Immunol. 2017 Jan 15;198(2):776-787. doi: 10.4049/jimmunol.1601585. Epub 2016 Dec 7. Erratum in: J Immunol. 2017 Jun 1;198(11):4547. PMID: 27927967; PMCID: PMC5225030.